The role of reinforced concrete roofs in the seismic performance of masonry buildings

The role of reinforced concrete roofs in the seismic performance of masonry buildings

Alessandro Cardoni[a], Gian Paolo Cimellaro[b,*]

[a]PhD Student, Department of Structural, Geotechnical and Building Engineering, Politecnico di Torino, Corso Duca degli Abruzzi 24, 10129, Turin, Italy. E-mail: alessandro.cardoni@polito.it

[b]Associate Professor, Department of Structural, Geotechnical and Building Engineering, Politecnico di Torino, Corso Duca degli Abruzzi 24, 10129, Turin, Italy. E-mail: gianpaolo.cimellaro@polito.it

[*]Corresponding author. Tel.: +39 011 0904801. E-mail: gianpaolo.cimellaro@polito.it

Abstract

The 2016 Central Italy earthquake caused many collapses of existing masonry buildings that had previously been retrofitted with reinforced concrete roofs. The aim of this paper is to explore the role of these roofs in the seismic behaviour of masonry buildings. Simple analytical models are presented to illustrate two typical out-of-plane collapse mechanisms: wall overturning and vertical flexure. The models are based on linear kinematic analysis, which allows fast modelling and calculation of a coefficient that can be used to assess the safety level of a structure. Nonlinear kinematic analyses were also performed. Both methods were applied to two case studies taken from areas struck by the earthquake. Results show that linear analysis represents an effective tool for preliminary verifications that can allow one to understand whether retrofit interventions are needed.

Keywords: masonry, reinforced concrete roof, collapse, retrofit, kinematic analysis, Central Italy earthquake

1. Introduction

After the 24th August 2016 Central Italy earthquake, most of the buildings of small towns nearby the epicenter were declared unsafe and several structures collapsed completely. Poor material quality and scant building techniques were certainly the main reason of collapses. However, inadequate retrofit interventions also contributed to the disruptive effect of the seismic event. For instance, the replacement of the old wooden roofs with reinforced concrete roofs seemed to facilitate some mechanisms that led to severe damages and collapses. This type of retrofitting was broadly adopted in the 80s and 90s since it was believed to be effective against seismic actions. In fact, it was the Italian code itself to recommend it [1] . Moreover, at that period there was a massive use of concrete that led to a gradual abandon of research and experimental tests on masonry [2] . The overall idea was to put robust structures such as RC roofs and floors connected to perimetric walls by means of RC ring beams to avoid independent movements of masonry macro-elements. After Tolmezzo earthquake in 1976, this and other retrofitting techniques became part of technical codes, until Umbria and Marche earthquake in 1997 [3, 4] .

This event pointed out the disadvantages of heavy and stiff roofs and floors. In fact, if vertical structures are not robust enough, they are indeed the primary cause of collapses. The significant stiffness and load increment at the top have led to the collapse of the walls, which were made of poor materials and not strengthened. Conversely, there were also many cases of masonry structures retrofitted with reinforced concrete roofs that withstood the earthquake with no significant damages (Figure 1).

Figure 1. Masonry buildings retrofitted with concrete roof not collapsed after the earthquake in Pescara del Tronto (a-b) and small villages near Accumoli (c-d).

However, there is no guarantee that those buildings are safe. Therefore, in this paper a simple verification procedure that is able to estimate the level of safety of masonry buildings with reinforced concrete roofs is implemented. The adopted approach is based on the linear kinematic analysis, which is also described by Italian codes [5, 6]. Despite the method is well known in its theoretical formulation, it is rarely used and usually the effect of the roof and the connection among structural elements are neglected. This research contributes to the current literature with practical applications of the kinematic analysis introducing simplified analytical models that take into account the effect of reinforced concrete roofs. An additional advantage of the proposed models is that the number of input parameters has been reduced as much as possible so that the analysis does not require any particular investigation or survey to be carried out. A safety factor was also defined to assess the safety level of the building towards different collapse

mechanisms. The choice of a simplified procedure has been made in order to have a fast tool which could be used even by non-professional users. The method would allow property owners to understand if they are in danger. For instance, if the obtained safety factor is low or close to the unsafe threshold, further investigations should be conducted. More detailed methods have been studied by many authors to describe masonry buildings behaviour, but they need to be calibrated and the input data are often not accessible [7-10]. Obviously, results will not be as accurate, and a certain margin of error should be taken into account in final considerations. Nonetheless, they can provide relevant preliminary information about the structure. In addition, in the literature there is a number of studies about masonry where analytical models turned out to be highly effective and close to the real behaviour [11, 12].

After defining the formulation, the method is applied to different models describing the overturning and the vertical flexural behaviour. The models derive from those commonly used to study the out-of-plane mechanisms [13-15] and the arch rocking [16-18]. To analyse the influence of the connection between the roof and the floor to the walls, a ring beam is also considered. The presence of a reinforced concrete (RC) ring beam is dangerous if it is not well connected to masonry walls and if the latter is not strengthened. Furthermore, the spread of reinforced concrete in the construction sector, led to wrong applications in the interventions of existing buildings. Nowadays there are many solutions to realize effective structural connections, such as reinforced masonry ring beams [19]. The use of innovative composite materials has become a common practice in retrofit strategies. Several studies have been carried out in this field which has allowed to investigate the behavior of strengthened beams [20, 21] and strengthened masonry walls through out-of-plane tests [22].

Two case studies taken from two towns struck by the abovementioned earthquake were analyzed, but the method can be extended to any building by choosing appropriate parameters. Both examples were selected by considering typical houses in the area, built with local materials and poor construction techniques and retrofitted with reinforced concrete roofs. The first one is 1-storey building while the second one has two storeys and thus also the action of the inter-storey floor is considered in the model. For each model, the linear kinematic analysis is repeated for different values of the input parameters, as they could be affected by uncertainty. In this way it is possible to see the influence of a single parameter and what happens if it is over-estimated or under-estimated. Finally, nonlinear analyses are performed in order to compare the results and understand if the additional computational effort of a more refined method is worth it.

2. The linear kinematic analysis

In existing masonry buildings there are often collapses due to a loss of equilibrium of some portions of bearing structures. In general, these types of mechanisms happen when seismic forces act in the out-of-plane direction. The linear kinematic analysis can be used to study these phenomena and for the verification process. It is based on the choice of the possible mechanisms that are most likely to happen. These ones are assumed by evaluating the current cracking state and analyses performed on similar buildings. In the literature there are plenty of studies on historical buildings, such as churches, which are helpful to clarify how the collapse process activates and evolve [23]. The ability to detect the most probable mechanisms is crucial to prevent local or global collapses, since it is possible to run specific analyses and consequently suggest specific interventions.

The linear kinematic approach schematizes the building in a discrete number of macro-elements which move according to their boundary conditions. For this reason, the assumptions are that the material has no tensile strength and infinite compressive strength. In each rigid block, vertical loads (including dead and external loads) and a system of horizontal forces are applied. Horizontal forces are proportional to the vertical loads through a coefficient called load multiplier (α). Incrementing the load multiplier, it is possible to evaluate the horizontal force that activates a specific mechanism. α_C is named the collapse load multiplier, and it is calculated with the principle of virtual works. Therefore, the total work of the external forces (L_e) has to be equal to the total work of the internal forces (L_i) which in this case is null as shown in Eq. (1):

$$L_e = \alpha_C \left(\sum_{i=1}^{n} W_i \cdot \delta_{x,i} + \sum_{j=n+1}^{n+m} W_j \cdot \delta_{x,j} \right) - \sum_{i=1}^{n} W_i \cdot \delta_{y,i} - \sum_{h=1}^{o} F_h \cdot \delta_h = L_i = 0 \quad (1)$$

where: n is the number of the weight forces applied to all macro-elements; m is the number of weight forces that generate horizontal forces upon macro-elements; o is the number of external forces; W_i is the generic weight force; W_j is the generic weight force that generates horizontal forces upon macro-elements; $\delta_{x,i}$ is the virtual horizontal displacement of the point where the i-th weight force is applied; $\delta_{y,i}$ is the virtual vertical displacement of the point where the i-th weight force is applied; F_h is the generic external force; δ_h is the virtual displacement of the point where the generic external force F_h is applied. Eq. (1) often becomes an equilibrium equation between a stabilizing moment and an overturning moment, so it is not necessary to calculate the virtual displacement. The method is also used to determine the most probable collapse mechanism which is the one that requires less energy to be activated (i.e. the one with the lower load multiplier). However, the decay conditions of masonry should never be neglected since they are able to reveal if a specific mechanism has already been activated. Once α_C is calculated, it is possible to obtain the acceleration that generates the mechanism (Eq. (2)).

$$a_0^* = \frac{\alpha_C \cdot \sum_{i=1}^{n+m} P_i}{M^* \cdot FC} \quad (2)$$

where FC is a coefficient that depends on the level of knowledge about the masonry structure. The level of knowledge is based on information like geometry, construction details, and material properties. Such data can be acquired in different ways, from generic research and visual inspection to extensive tests and measurements. Since the material strength is not considered in this research, only basic information about geometric characteristics, type of masonry panels and construction details was collected. According to the Italian code [6], three level of knowledge can be identified: limited, extended and exhaustive. Due to the limited available data, the level of knowledge is limited. In this case, the code reports the FC coefficient has to be assumed equal to 1,35 which reduces the acceleration that generates the mechanism. M^* is the participating mass, calculated considering the virtual displacements of the points where the loads are applied, as shown in Eq. (3) [6]:

142 $$M^* = \frac{\left(\sum_{i=1}^{n+m} P_i \cdot \delta_{x,i}\right)^2}{g \cdot \sum_{i=1}^{n+m} P_i \cdot \delta_{x,i}^2} \quad (3)$$

143 The acceleration given by Eq. (2) has now to be compared with an allowable acceleration.
144 This one is given by Eq. (4), which is valid when the analysed blocks are in contact with the
145 ground, meaning that the mechanism involves ground floor walls:

146 $$a^* = \frac{a_g \cdot S}{q} \quad (4)$$

147 where: a_g is the peak ground acceleration at the site determined, as indicated by Italian codes,
148 for a return period of 475 years; q is the reduction factor which can be assumed equal to 2 for
149 regular masonry structures; S is given by the product of two coefficients: S_s that depends on
150 the soil category and represents the stratigraphic amplification, and S_t which takes into
151 account the effects of the topographical amplification and depends on the surface
152 configuration of the soil.

153 It is clear that the acceleration that activates the mechanism should be greater than the
154 allowable one. To quickly verify this, it is possible to introduce a safety factor which is the
155 ratio between the two accelerations (Eq. (5)):

156 $$SF = \frac{a_0^*}{a^*} \geq 1 \quad (5)$$

157

158 ## 3. Analytical models

159 In some cases, there are mechanisms that are suggested by the building itself just looking to
160 the geometry, the nature of the structural elements, the cracking state, the interventions
161 occurred over the years, etc. The linear kinematic analysis is a powerful tool that can be used
162 to describe local mechanisms that have been observed after disruptive earthquakes. If only
163 out-of-plane mechanisms are considered, then they can be basically grouped in three
164 categories: (i) overturning, (ii) vertical flexural behaviour and (iii) horizontal flexural
165 behaviour. In this paper only the first two categories are considered since they were the main
166 cause of collapses during the Central Italy earthquake. In addition, for these two mechanisms
167 the presence of a reinforced concrete roof is more crucial. For the overturning, two cases
168 were studied, a 1-storey and a 2-storey building, whereas for the vertical flexural behaviour
169 only the 2-storey building was studied, taking into account also the effect of the inter-storey.
170 The considered macro-elements are the walls, the floor, and the reinforced concrete roof. This
171 one is assumed as an element that transfers only vertical loads to the walls and no lateral
172 thrusts. Therefore, it is modelled as a rigid block with a large mass. The effects of
173 perpendicular walls are neglected, as in many real cases there are no connections. All models
174 consider alternatively the presence and the absence of connections between roof and walls
175 (by means of a ring beam) and between floor and walls. When there is a ring beam the roof is
176 fixed to the walls and moves with them, while when there is no connection the roof is
177 considered simply supported.

3.1 1-storey overturning without ring beam

This is the case of simple overturning where there is no ring beam, and therefore no connection between the top of the wall and the roof. For this reason, the macro-elements are independent one from another and only one wall is subjected to overturning. Figure 2 illustrates the mechanism and the forces involved. W_1 is the weight of the left wall, P_R is the weight of the roof applied in its center of mass G_R and split equally between the two walls.

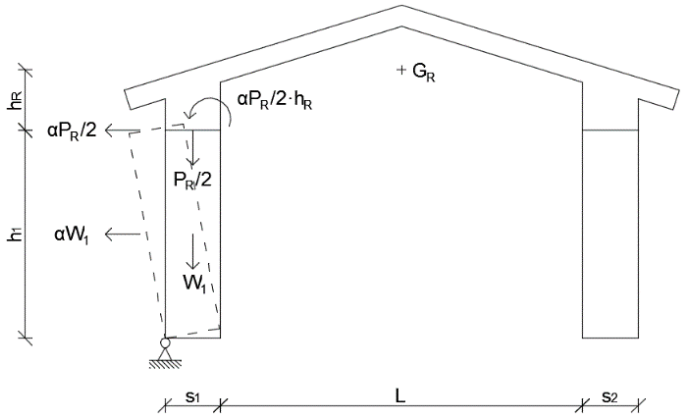

Figure 2. Calculating scheme for 1-storey overturning without ring beam.

According to Eq. (1) the load multiplier that leads to collapse for this configuration is given by Eq. (6):

$$\alpha_C = \frac{W_1 \cdot \frac{s_1}{2} + \frac{P_R}{2} \cdot \frac{s_1}{2}}{W_1 \cdot \frac{h_1}{2} + \frac{P_R}{2} \cdot \left(h_1 + h_R\right)} \tag{6}$$

where s_1 is the thickness of left wall; h_1 is the height of walls; h_R is the distance between the top of walls and the center of mass (G_R) of the roof, and L is the span length.

3.2 1-storey overturning with ring beam

If there is a ring beam the two external walls are connected at the top to realize the so called "box-like" behaviour. Macro-elements are no more independent, so they move together until the loss of equilibrium. As shown in Figure 3 both walls rotate around the hinge at the bottom under a seismic action. The effect of the ring beam is modelled using a force acting in the opposite direction of the kinematic movement. To a first approximation, it can be calculated as the product of the friction coefficient μ and the weight of the roof P_R. For the estimation of the friction coefficient there are many experimental tests available in literature [24]. However, since the proposed model is simplified and no detailed information about the materials were available, the guidelines provided by national codes were followed [5, 6]. In particular, as a precautionary measure, a friction coefficient of 0.4 was used, which is the lowest among the suggested values.

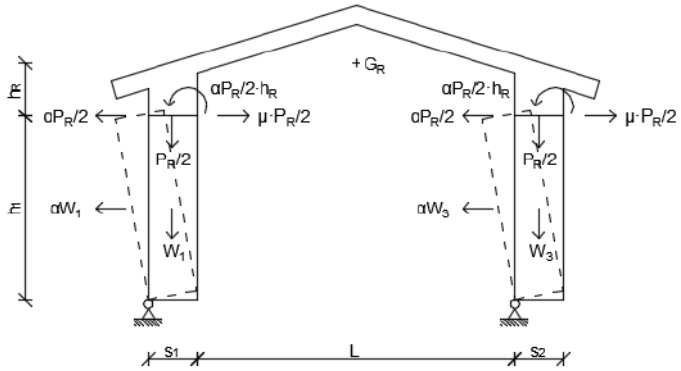

Figure 3. Calculating scheme for 1-storey overturning with ring beam.

Eq. (7) gives the collapse load multiplier in the case of overturning with ring beam:

$$\alpha_C = \frac{\left(W_1 + \frac{P_R}{2}\right)\cdot\frac{s_1}{2} + \left(W_3 + \frac{P_R}{2}\right)\cdot\frac{s_2}{2} + \left(\mu\cdot P_R\right)\cdot h_1}{\left(W_1 + W_3\right)\cdot\frac{h_1}{2} + P_R\cdot\left(h_1 + h_R\right)} \tag{7}$$

where s_1, s_2 are the thicknesses of left and right walls, respectively; W_1 is the weight of the left wall, while W_3 is the weight of the right one.

3.3 2-storey overturning without ring beam

This model is an extension of the 1-storey model, so the same assumptions can be made. However, in this model there is a new macro-element, the floor of weight P_F that is split equally between the left and the right wall. In a simplified manner, in the current model and the ones below, the contact area between the inter-storey floor and ground floor walls is assumed to be half the thickness of walls. To allow a complete rotation of the two masonry panels, the floor is considered disconnected to the walls and the connection to the ground is modelled as a hinge (Figure 4). The formulation of the load multiplier α_C is given by Eq. (8):

$$\alpha_C = \frac{\left(W_1 + W_2 + \frac{P_R}{2}\right)\cdot\frac{s_1}{2} + \frac{P_F}{2}\cdot\frac{3s_1}{4}}{W_1\cdot\frac{h_1}{2} + \frac{P_F}{2}\cdot h_1 + W_2\cdot\left(h_1 + \frac{h_2}{2}\right) + \frac{P_R}{2}\cdot\left(h_1 + h_2\right) + \frac{P_R}{2}\cdot h_R} \tag{8}$$

where W_2 is the weight of the left masonry panel of the upper level and h_2 is its height.

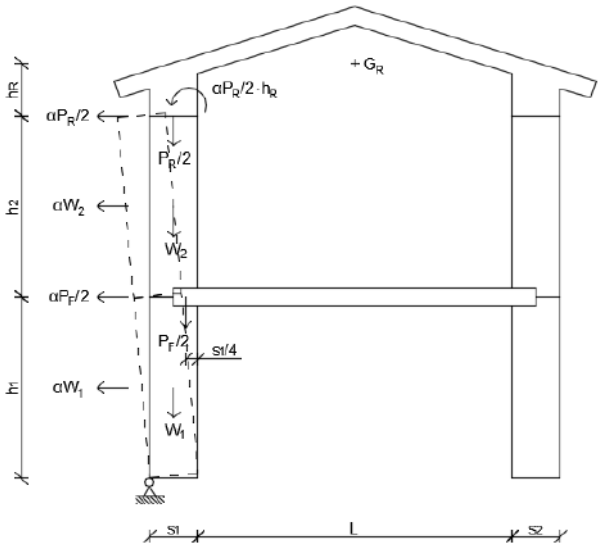

225

226 Figure 4. Calculating scheme for 2-storey overturning without ring beam.

227

228 **3.4 2-storey overturning with ring beam**

229 As already seen in the 1-storey case, the ring beam at the roof level connects the walls
230 together, so they can overturn at the same time. Once again, the connection is modelled as a
231 friction force proportional to the weight of the roof (Figure 5). In this case, the inter-storey
232 floor is well connected to the walls and moves together with them. Eq. (9) provides the
233 collapse load multiplier for this case:

234
$$\alpha_C = \frac{\left(W_1 + W_2 + \frac{P_R}{2}\right)\cdot\frac{s_1}{2} + \frac{P_F}{2}\cdot\frac{3s_1}{4} + \left(W_3 + W_4 + \frac{P_R}{2}\right)\cdot\frac{s_2}{2} + \frac{P_F}{2}\cdot\frac{s_2}{4} + (\mu\cdot P_R)\cdot(h_1 + h_2)}{(W_1 + W_3)\cdot\frac{h_1}{2} + P_F\cdot h_1 + (W_2 + W_4)\cdot\left(h_1 + \frac{h_2}{2}\right) + P_R\cdot(h_1 + h_2) + P_R\cdot h_R} \quad (9)$$

235 where W_4 is the weight of the right masonry panel of the upper level.

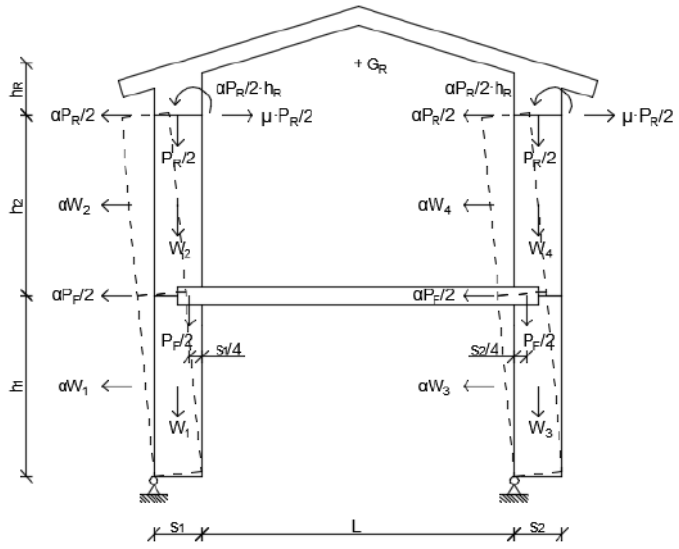

236

237 Figure 5. Calculating scheme for 2-storey overturning with ring beam.

3.5 2-storey flexural behaviour without connection between floor and walls

Vertical flexural behaviour can occur in any part of the wall. It can be seen as a triple-hinged arch where, in this specific case, the hinges are located at the bottom, at the top, and at the inter-storey level. This means that the mechanism is activated by the horizontal inertial force caused by the floor during the seismic action. The upper level wall is connected at the top of the roof, whereas the inter-storey floor is not connected to the walls (Figure 6). The collapse load multiplier α_C is given by Eq. (10):

$$\alpha_C = \frac{W_1 \cdot \frac{s_1}{2} + W_2 \cdot \left(s_1 + \frac{s_1}{2} \cdot \frac{h_1}{h_2} \right) + \frac{P_F}{2} \cdot \frac{3s_1}{4} + \frac{P_R}{2} \cdot \left(s_1 + \frac{s_1}{2} \cdot \frac{h_1}{h_2} \right)}{W_1 \cdot \frac{h_1}{2} + W_2 \cdot \left(h_1 \cdot \frac{h_1}{h_2} + \frac{h_2}{2} \cdot \frac{h_1}{h_2} \right) + \frac{P_F}{2} \cdot h_1} \tag{10}$$

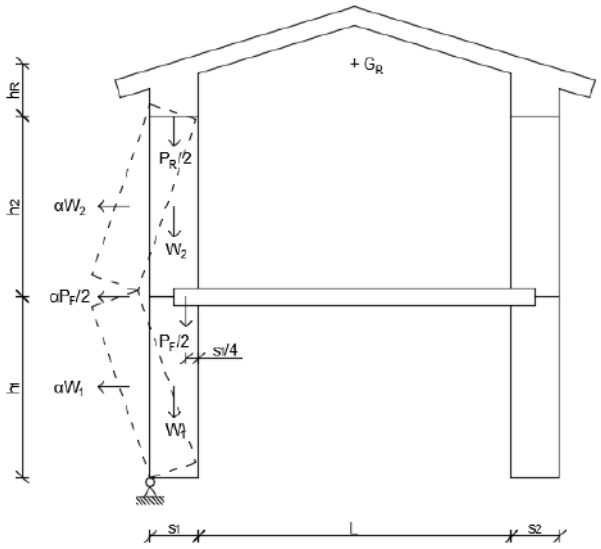

Figure 6. Calculating scheme for vertical flexural behaviour without floor-walls connection.

3.6 2-storey flexural behaviour with connection between floor and walls

In this model the floor is well connected to the walls so that it can pull them together, but eventually it detaches. To represent this type of connection, a friction force proportional to the floor weight is considered at the inter-storey level (Figure 7).

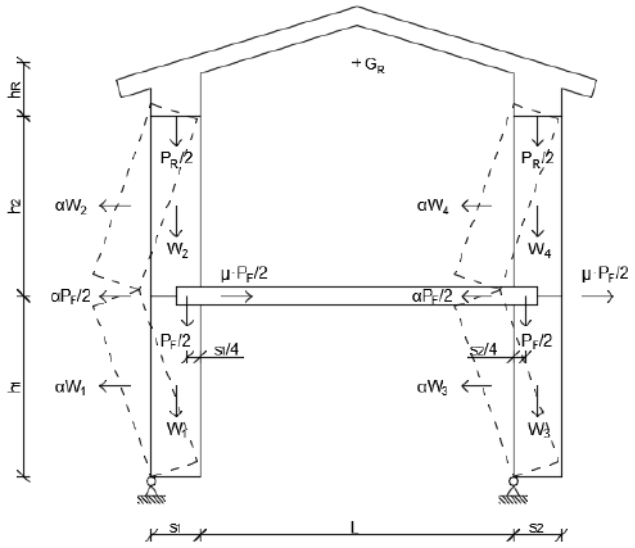

Figure 7. Calculating scheme for vertical flexural behaviour with floor-walls connection.

Eq. (11) allows to get the collapse load multiplier for this model:

$$\alpha_C = \frac{W_1 \cdot \frac{s_1}{2} + W_2 \cdot \left(s_1 + \frac{s_1}{2} \cdot \frac{h_1}{h_2} \right) + W_3 \cdot \frac{s_2}{2} + W_4 \cdot \left(s_2 + \frac{s_2}{2} \cdot \frac{h_1}{h_2} \right) + \frac{P_F}{2} \cdot \frac{3s_1}{4} + \frac{P_F}{2} \cdot \frac{s_2}{4}}{\left(W_1 + W_3 \right) \cdot \frac{h_1}{2} + \left(W_2 + W_4 \right) \cdot \left(h_1 \cdot \frac{h_1}{h_2} + \frac{h_2}{2} \cdot \frac{h_1}{h_2} \right) + P_F \cdot h_1} + \\ + \frac{\frac{P_R}{2} \cdot \left(s_1 + \frac{s_1}{2} \cdot \frac{h_1}{h_2} \right) + \frac{P_R}{2} \cdot \left(s_2 + \frac{s_2}{2} \cdot \frac{h_1}{h_2} \right) + \left(\mu \cdot P_F \right) \cdot h_1}{\left(W_1 + W_3 \right) \cdot \frac{h_1}{2} + \left(W_2 + W_4 \right) \cdot \left(h_1 \cdot \frac{h_1}{h_2} + \frac{h_2}{2} \cdot \frac{h_1}{h_2} \right) + P_F \cdot h} \tag{11}$$

4. Case studies

4.1 Pescara del Tronto case study

Figure 8 shows a house in Pescara del Tronto completely collapsed after the 2016 Central Italy earthquake, which can be used as an example to apply the 1-storey model. The data that were used as input in the model are the following: wall thickness ($s = s_1 = s_2$) = 0.4 m; roof thickness (s_R) = 0.15 m; wall height (h_1) = 3 m; wall length (l_w) = 7 m; span length (L) = 5 m; distance between the center of mass of the roof and the top of the wall (h_R) = 0.4 m; specific weight of masonry (P_m) = 19 kN/m^3; specific weight of reinforced concrete (P_c) = 21 kN/m^3; friction coefficient roof – wall (μ) = 0.4; PGA for a return period of 475 years (a_g) = 2.489 m/s^2; S_s = 1 (rock soil); S_t = 1.2 (top of a hill). The weight of the walls was calculated as $W_i = h_i \cdot l_w \cdot s_i \cdot P_m$, where *i=1, 2*, while the weight of the roof as

$$W_i = 2 \cdot \left[\sqrt{\left(s + L/2 \right)^2 + h_r^{\,2}} \cdot l_w \cdot s_r \cdot P_c \right].$$

Figure 8. View of the building used as case study before and after the earthquake.

As already mentioned, most of the data are geometrical so they can be easily collected. Only the PGA needs to be calculated referring to the information given by the Italian code [5]. In this case, the location is fixed, so the value can be determined analytically. The value used for S_s is referred to rock soil, while the one used for S_t is referred to the top of a hill as there is evidence of a slope behind the building.

4.1.1 Pescara del Tronto results

The results using the linear kinematic analysis and verification are reported in Table 1.

Table 1. Collapse load multipliers and safety factors for the Pescara del Tronto case study.

	1-storey overturning without ring beam	1-storey overturning with ring beam
α_C	0.10	0.26
SF	0.57	1.48

Comparing the load multipliers, it can be observed that the first mechanism is more likely to happen as the 1-storey overturning with ring beam case has a collapse load 2.6 times higher than the 1-storey overturning without ring beam. This is confirmed by the fact that the safety factor in the case without ring beam is lower and it is below the safety threshold. Indeed, as shown in Figure 8 there is no connection between roof and walls. If this kind of analysis was carried out in a pre-earthquake situation, it would have been possible to demonstrate how the building was unsafe towards a seismic event with a return period of 475 years. The actual demand of 2016 earthquake was larger than the one used as input for this verification procedure. However, the aim of the method is to report if retrofitting is needed to improve the level of safety. Validation analyses were not performed at this stage, but adequate interventions could have likely prevented the structure from a complete collapse.

A sensitivity analysis was carried out to assess the impact of the chosen input parameters on results. Most relevant outcomes were then plotted in graphs with the varying parameter on the *x* axis and the safety factor *SF* on the *y* axis. Figure 9(a) shows that when there is no

300 friction the two mechanisms are equivalent because of the symmetry of the systems and the
301 configuration is unsafe. The minimum friction coefficient to ensure a safety factor greater
302 than 1 is 0.2. As predictable, the impact of the friction is overall positive: it is enough to build
303 a ring beam able to ensure a friction coefficient of 0.4 and triple the safety factor. In Figure
304 9(b) the span length is varying, resulting in an increase or decrease in the weight of the roof.
305 This has almost no effects in the case without ring beam, which remains unsafe in the whole
306 range of variation. On the other hand, since the friction force is proportional to the weight of
307 the roof, increasing the span length leads to a significant increment of the safety factor. When
308 the masonry specific weight of the masonry varies, safety factor remains almost constant
309 (Figure 9(c)). The weight of the walls has indeed a twofold effect since it contributes to both
310 stabilizing and overturning forces. Also, looking at the equations that lead to determine SF (in
311 particular Eqs. (6-7) and Eq. (2)), it can be noticed how the weight appears always at both
312 nominator and denominator. Therefore, in the calculation steps its variation tends to have
313 negligible effects. Figure 9(d) shows the influence of the wall thickness. In the first case,
314 without ring beam, an increment of the wall thickness corresponds to a linear and
315 considerable increment of the *SF*. However, almost 70 cm walls are required to be in the safe
316 area. In the second case, there is an asymptotic trend. It means that for low thicknesses the
317 presence of the ring beam is effective (e.g. for s = 20 cm the *SF* is two times the *SF* in the
318 case with no ring beam), but for high thicknesses the structure is so massive that the presence
319 of the ring beam at the top is irrelevant. Finally, in Figure 9(e) different soil categories are
320 taken into account by varying the abovementioned parameter S_s. Following the guidelines
321 provided by the Italian seismic codes, the possible values S_s can assume were calculated
322 (Table 2). A rock soil allows to have higher safety factors, whereas if the quality gets worse
323 there is a decreasing trend, except for category E (coarse soil upon a stiff or soft soil).

324

325 Table 2. Values of the parameter S_s for different soil categories.

Soil category	**Description**	S_s
A	Rock soil (Vs30 > 800 m/s)	1.00
B	Soft rock and very dense soil (360 m/s < Vs30 < 800 m/s)	1.16
C	Stiff soil (180 m/s < Vs30 < 360 m/s)	1.33
D	Soft soil (Vs30 < 180 m/s)	1.48
E	Coarse soil upon stiff or soft soil	1.33

326

327

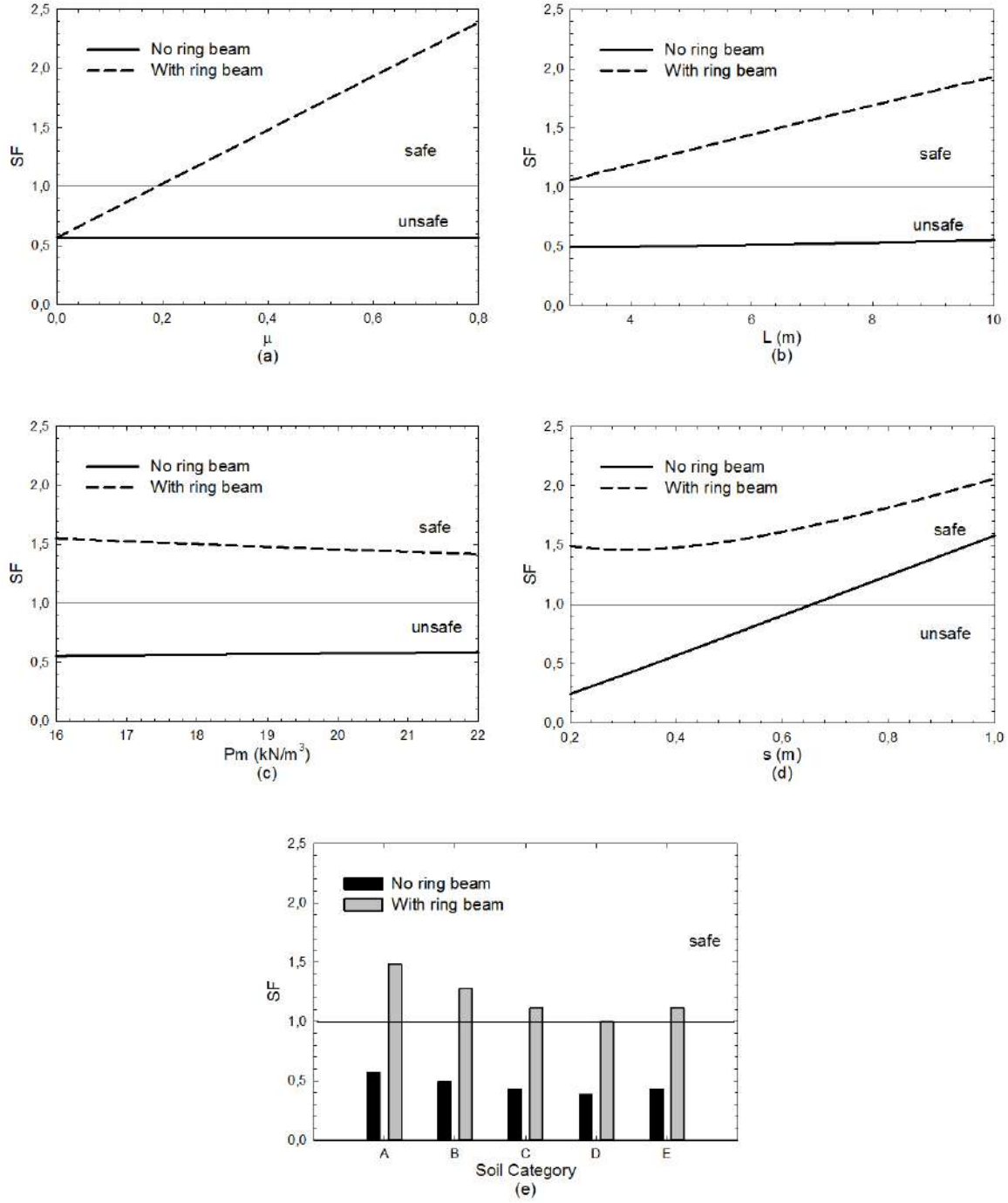

Figure 9. (a) Friction coefficient vs. safety factor, (b) span length vs. safety factor, (c) masonry specific weight vs. safety factor, (d) wall thickness vs. safety factor, (e) soil category vs. safety factor.

4.2 Amatrice case study

The 2-floor models were tested through the building in Figure 10 which was located in Amatrice. The data used as input for the analysis are the following: wall thickness ($s_1 = s_2$): 0.4 m; roof thickness (s_R): 0.15 m; wall height ($h_1 = h_2$): 3 m; wall length (l_w): 11 m; span length (L): 6.5 m; distance between the center of mass of the roof and the top of the wall (h_R):

0.4 m; specific weight of the masonry (P_m): 19 kN/m^3; specific weight of the reinforced concrete (P_c): 21 kN/m^3; floor weight (P_f): 4 kN/m^2; friction coefficient roof – wall (μ): 0.4; friction coefficient floor – wall (μ): 0.5; PGA for a return period of 475 years (a_g): 2.538 m/s^2; S_s: 1 (rock soil); S_t: 1 (flat area).

Figure 10. View of the building used as case study before and after the earthquake.

4.2.1 Amatrice results

The results obtained using the linear kinematic analysis are summarized in Table 3:

Table 3. Collapse load multipliers and safety factors for the Amatrice case study.

	2-storey overturning without ring beam	2-storey overturning with ring beam	2-storey vertical flexural behaviour without connection between floor and walls	2-storey vertical flexural behaviour with connection between floor and walls
α_C	0.06	0.16	0.16	0.27
SF	0.44	1.14	1.03	1.70

Comparing these results, it is clear that the configuration of overturning with no ring beam is the less safe and the most probable. The presence of a ring beam increases the collapse load multiplier of about 2.7 times for the overturning mechanism. On the other hand, the model with connection at the top of the walls and at floor level is the safest and less probable case. For the vertical flexural behaviour, the case with connection between floor and walls has 1.7 times as high of a collapse load as the case without connection has. Finally, it is possible to observe that the mechanisms of overturning with ring beam and vertical flexural behaviour without connection at floor level are almost equivalent.

Also for this case study, sensitivity analyses were performed for all parameters. The trends of variation of other parameters are really similar to the previous ones, thus the considerations done for the 1-storey model are still valid. The substantial difference between 2-storey overturning and vertical flexural behaviour is that in the second case the safety factors are higher. Omitting obvious and well-known results, it is worth to comment what happens when the floor weight is changing (Figure 11). In both cases of overturning and in the case of

vertical flexural behaviour without connection, when the floor weight varies the safety factor is not subject to significant changes. A slight reduction of SF can be observed in the overturning scenario for the model with ring beam as the floor weight increases. A heavier floor leads to greater horizontal inertial forces which contribute to the overturning. Instead, for the mechanism of vertical flexural behaviour with connection, a heavy floor has a positive impact since the stabilizing force increases. As far as the variation of soil category is concerned, the values of the S_s coefficient that were used in the previous case study are still valid (Table 2). It is interesting to notice that if the category of soil was not "A" (rock soil), then only the mechanism of vertical flexural behaviour with connection would be safe (Figure 12).

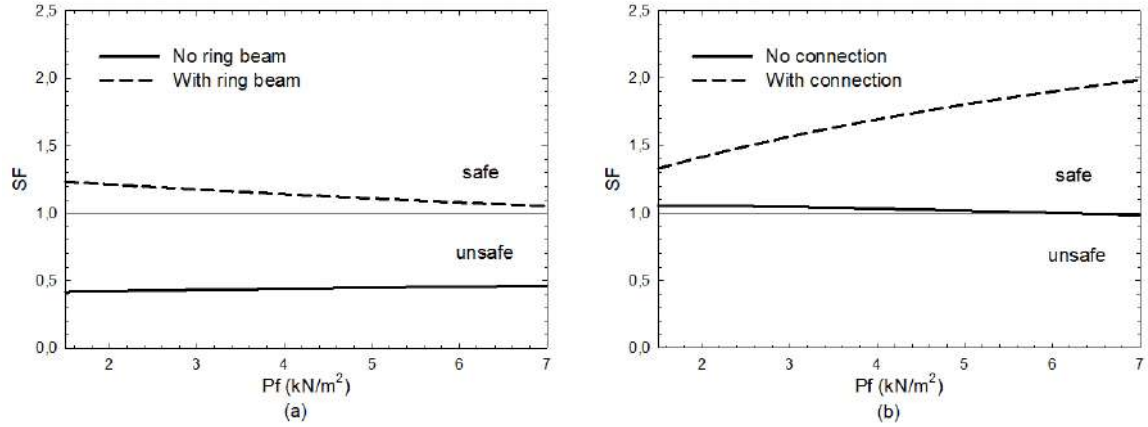

Figure 11. Floor weight vs. safety factor for the (a) overturning mechanism and the (b) vertical flexural behaviour.

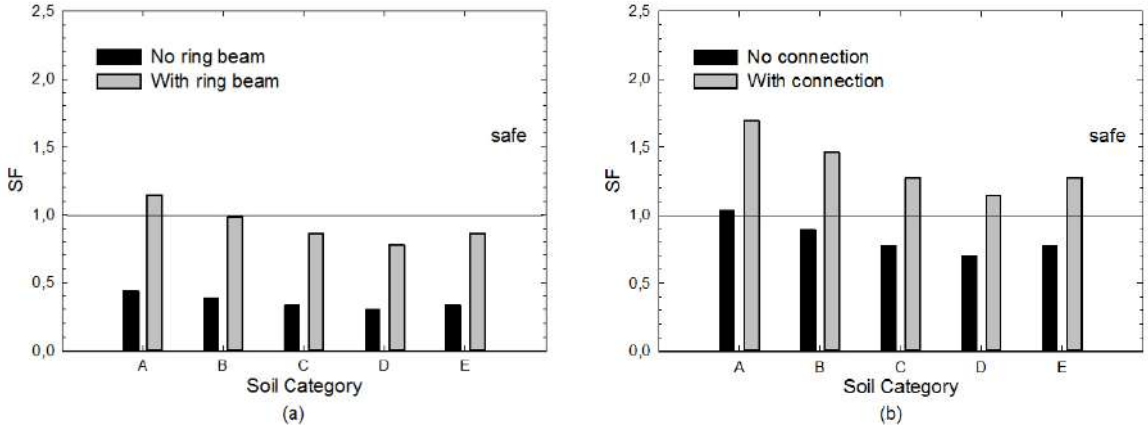

Figure 12. Soil category vs. safety factor for the (a) overturning mechanism and the (b) vertical flexural behaviour mechanism.

5. Nonlinear kinematic analysis

Nonlinear kinematic analyses were carried out with the aim of supporting the results obtained from linear analyses. The whole procedure follows the method proposed by Italian codes [5,

6], which is presented hereafter just in its main steps. The underlying idea of the method is to determine the trend of the horizontal action that the structure is progressively able to withstand during the collapse mechanism's evolution. This can be seen as the capacity curve of an equivalent single degree of freedom system. The ultimate displacement capacity of the local mechanism is then defined and compared with the seismic demand. Similarly to the linear case, a multiplier α is introduced and defined as the ratio between the applied horizontal forces and the displacement d_k of a control point. The horizontal multiplier of loads is evaluated at various configurations of the kinematic chain until reaching the collapse condition, which is identified by a null multiplier α, and a displacement $d_{k,0}$. Assuming that involved actions (i.e. weights, external and internal forces) are constant during the evolution of the mechanism, the curve is almost linear. In this case, only the evaluation of the displacement $d_{k,0}$ is required, and the curve is described by Eq. (12):

$$\alpha = \alpha_0 (1 - d_k / d_{k,0}) \tag{12}$$

where α_0 denotes the value of the multiplier capable of activating the analysed mechanism. The problem can be solved considering a configuration varied from the static condition and calculating the induced finite rotation θ_k by means of virtual work principle. Reaching the collapse situation, the overturning moment equals the stabilizing moment, and the resulting nonlinear equation gives the final rotation $\theta_{k,0}$. Once the latter is determined, the corresponding displacement $d_{k,0}$ can be obtained. Let the control point be the center of gravity of vertical forces, and h_{bar} be its distance from the base hinge. Eq. (13) expresses the relation between the rotation angle and the displacement of the control point related to ultimate capacity towards horizontal actions.

$$d_{k,0} = h_{bar} sin\theta_{k,0} \tag{13}$$

At this point, it is possible to define the α - d_k curve according to Eq. (12). The equivalent capacity curve should now be determined. It describes the relation between the acceleration a^* that activates the mechanism and displacement d^*. The first is obtained through Eq. (2) as in the linear case, whereas d^* is given by Eq. (14).

$$d^* = d_{k,0} \frac{\sum_{i=1}^{n+m} P_i \delta_{x,i}^2}{\delta_{x,k} \sum_{i=1}^{n+m} P_i \delta_{x,i}} \tag{14}$$

where: $n+m$ is the number of weight forces that generates horizontal forces upon the macro-elements; P_i is the generic weight force; $\delta_{x,i}$ is the virtual horizontal displacement of the application point of P_i; $\delta_{x,k}$ is the horizontal virtual displacement of the control point.

Making the same assumption done for the α - d_k curve, the capacity curve can be derived from Eq. (15).

$$a^* = a_0^* (1 - d^* / d_0^*) \tag{15}$$

where d_0^* is the equivalent displacement corresponding to $d_{k,0}$.

The verification for the life safety limit state consists in a comparison between the ultimate displacement capacity d_u^* of the local mechanism and the spectral displacement evaluated at the period T_s (Eq. (16)):

$$T_s = 2\pi\sqrt{\frac{d_s^*}{a_s^*}} \tag{16}$$

where a_s^*, is the acceleration correspondent to the displacement d_s^*, which is equal to $0.4d_u^*$, and $d_u^* = 0.4d_0^*$. Therefore, if d_u^* is greater than the spectral displacement $S_{De}(T_s)$, the verification is fulfilled (Eq. (17)).

$$SF = \frac{d_u^*}{S_{De}(T_s)} \geq 1 \tag{17}$$

Table 4 shows obtained results for all analysed models. As expected, a lack of connection is responsible of a small safety factor, always around 1 for the three studied cases. On the other hand, the presence of a ring beam or floor-wall connections ensures much more capacity to withstand larger ultimate displacements, which also means a higher safety level. The difference is less exaggerated in the case of vertical flexural behaviour since the connection between the floor and the wall makes the structure more rigid.

Comparing the linear with the nonlinear kinematic analysis in terms of safety factors, the bar chart of Figure 13 can be plotted. The nonlinear kinematic analysis usually provides safety coefficients that are two times or more the coefficient obtained with the linear analysis. This confirms that a fast and preliminary analysis, such as the linear one, provides precautionary results and it is recommended to understand if further investigations are needed. The described trend is inverted in the cases of vertical flexural behaviour, although the nonlinear safety factors are just slightly lower than linear ones. This phenomenon is due to the fact that the weight of a reinforced concrete roof has a particularly positive effect for these two models. In addition, the same analyses were repeated several times increasing the weight of the roof for each iteration. In all cases the safety factor increased, but the increment in the linear analysis was greater than in the nonlinear one.

Table 4. Results of the nonlinear kinematic analysis.

	Pescara del Tronto		**Amatrice**			
	1-storey overturning without ring beam	**1-storey overturning with ring beam**	**2-storey overturning without ring beam**	**2-storey overturning with ring beam**	**2-storey flexural behaviour without connection**	**2-storey flexural behaviour with connection**
d_u^* **[m]**	0.089	0.227	0.093	0.326	0.041	0.074
SF	1.04	2.66	1.02	3.02	1.12	1.95

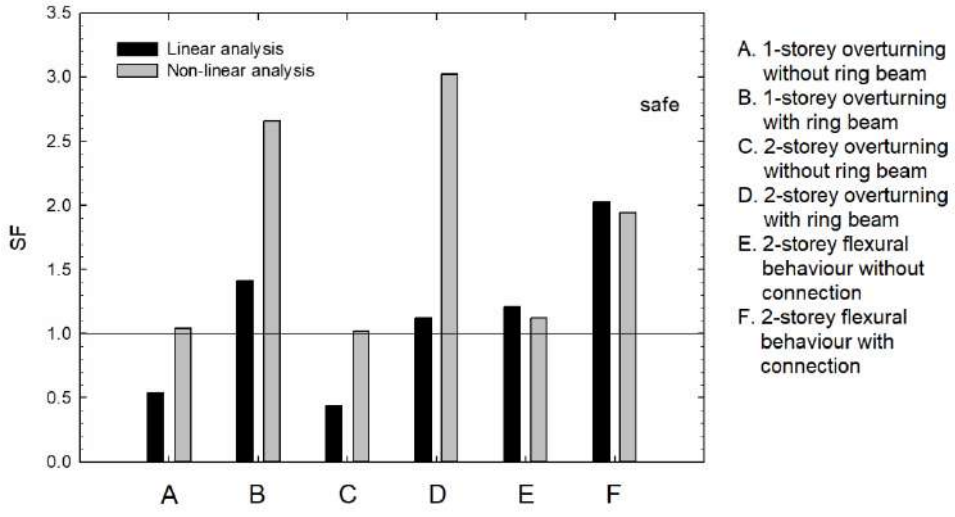

Figure 13. Comparison between safety factors resulting from linear and non-linear analyses.

6. Conclusions

The 2016 Central Italy earthquake caused damages and collapses of many masonry buildings, including those retrofitted with reinforced concrete roofs. This type of retrofit intervention seems to facilitate some collapse mechanisms if not properly executed. The paper presents a simplified procedure to evaluate the seismic performance of masonry buildings retrofitted with reinforced concrete roofs based on the linear kinematic analysis. Despite the analysis method is well known, the proposed models have the advantage of explicitly considering the interaction between the roof and the walls. Moreover, they require only few input parameters that can be easily obtainable. The collapse load multiplier obtained as output of the linear kinematic analysis was used to define a safety factor to have an idea whether a structure can be considered safe towards a certain collapse mechanism.

The introduced analytical models are based on the overturning and vertical flexural behaviour collapse mechanisms. In particular, the overturning scenario was analysed both for a 1-storey and a 2-storey building, while the vertical flexural behaviour was considered for a 2-storey building. Each scenario is studied twice: one configuration assuming that there is no connection among the involved macro-elements and another one that provides for an effective connection. The resulting six models were applied to two case studies, a 1-storey and a 2-storey building both collapsed during the 2016 Central Italy earthquake. Results highlight the importance of an efficient connection between the reinforced concrete roof and masonry walls and that some configurations are unsafe, which means additional investigations and possibly retrofit intervention are required. To account for the uncertainties introduced by the simplified models, sensitivity analyses were performed. These allowed to evaluate the influence of each input parameter to the overall safety level of the structure, highlighting peculiar aspects in each mechanism. Nonlinear kinematic analyses were also carried out and results were compared to those obtained from linear analyses. It was possible to observe that the linear analysis is faster and more precautionary as it provides smaller safety factors with respect to the nonlinear one.

Overall, the proposed analytical models represent an effective yet simple tool that can serve as a preliminary evaluation of the safety level of masonry structures retrofitted with reinforced concrete roofs. The method is not meant to be an alternative to other more refined analyses, such as finite element methods, that would allow for a more accurate safety verification. However, due to its simplicity, the procedure could be recommended when only few input data are available and be applied even by non-professional users to understand if further investigations and/or retrofit interventions are needed.

Acknowledgement

The research leading to these results has received funding from the European Research Council under the Grant Agreement n. ERC_IDEAL RESCUE_637842 of the project IDEAL RESCUE_Integrated Design and Control of Sustainable Communities during Emergencies.

References

[1] "DM 16-01-1996. Norme tecniche per le costruzioni in zone sismiche". 1996. Ministero dei Lavori Pubblici: Gazzetta Ufficiale.

[2] Calderini, C. 2008. "Use of reinforced concrete in preservation of historic buildings: conceptions and misconceptions in the early 20th century". *International Journal of Architectural Heritage*, 2(1): 25-59.

[3] Dolce, M., A. Masi, and A. Goretti. 1999. *Damage to buildings due to 1997 Umbria-Marche earthquake*. Seismic Damage to Masonry Buildings, ed. A. Bernardini. Leiden: A a Balkema Publishers. 71-80.

[4] Donati, S., F. Marra, and A. Rovelli. 2001. "Damage and ground shaking in the town of Nocera Umbra during Umbria-Marche, central Italy, earthquakes: The special effect of a fault zone". *Bulletin of the Seismological Society of America*, 91(3): 511-519.

[5] "DM 14-01-2008. Norme tecniche per le costruzioni". 2008. Ministero dei Lavori Pubblici: Gazzetta Ufficiale.

[6] "Circolare 2 febbraio 2009, n. 617 Istruzioni per l'applicazione delle «Nuove norme tecniche per le costruzioni»". 2009. Ministero delle Infrastrutture e dei Trasporti.

[7] Chen, Z.X., et al. 2016. "Nonlinear Analysis of Masonry Buildings Under Seismic Actions with a Multifan Finite Element". *International Journal of Structural Stability and Dynamics*, 16(1).

[8] Valente, M. and G. Milani. 2016. "Non-linear dynamic and static analyses on eight historical masonry towers in the North-East of Italy". *Engineering Structures*, 114: 241-270.

[9] Milani, G. 2011. "Simple lower bound limit analysis homogenization model for in- and out-of-plane loaded masonry walls". *Construction and Building Materials*, 25(12): 4426-4443.

[10] Milani, G. and M. Valente. 2015. "Comparative pushover and limit analyses on seven masonry churches damaged by the 2012 Emilia-Romagna (Italy) seismic events: Possibilities of non-linear finite elements compared with pre-assigned failure mechanisms". *Engineering Failure Analysis*, 47: 129-161.

[11] Arcidiacono, V., G.P. Cimellaro, and J.A. Ochsendorf. 2015. “Analysis of the failure mechanisms of the basilica of Santa Maria di Collemaggio during 2009 L'Aquila earthquake”. *Engineering Structures*, 99: 502-516.
[12] Arcidiacono, V., et al. 2016. “The Dynamic Behavior of the Basilica of San Francesco in Assisi Using Simplified Analytical Models”. *International Journal of Architectural Heritage*, 10(7): 938-953.
[13] Casapulla, C. and A. Maione. 2011. “Out-of-plane local mechanisms in masonry buildings. the role of the orientation of horizontal floor diaphragms”. *Proceedings of the 9th Australasian Masonry Conference*: 225-235.
[14] Costa, A.A., et al. 2012. “Out-of-plane behaviour of existing stone masonry buildings: experimental evaluation”. *Bulletin of Earthquake Engineering*, 10(1): 93-111.
[15] Guadagnuolo, M., A. Donadio, and G. Faella. 2012. *Out-of-plane failure mechanism of masonry building corners*. Structural Analysis of Historical Constructions, Vols 1-3., ed. J. Jasienko. Structural Analysis of Historical Constructions, Vols 1-3. 481-488.
[16] Makris, N. 2014. “The role of the rotational inertia on the seismic resistance of free-standing rocking columns and articulated frames”. *Bulletin of the Seismological Society of America*, 104(5): 2226-2239.
[17] Makris, N. and M.F. Vassiliou. 2014. “Dynamics of the rocking frame with vertical restrainers”. *Journal of Structural Engineering*, 141(10): 04014245.
[18] Giresini, L., M. Fragiacomo, and M. Sassu. 2016. “Rocking analysis of masonry walls interacting with roofs”. *Engineering Structures*, 116: 107-120.
[19] Borri, A., G. Castori, and A. Grazini. 2009. “Retrofitting of masonry building with reinforced masonry ring-beam”. *Construction and Building Materials*, 23(5): 1892-1901.
[20] Guadagnuolo, M. and G. Faella. 2015. “Floor masonry beams reinforced by BFRG Innovation on advanced composite materials for strengthening of masonry structures”, in *XIII Forum Internazionale di Studi “Le Vie dei Mercanti”–HERITAGE and TECHNOLOGY MIND KNOWLEDGE EXPERIENCE*. La scuola di Pitagora editrice, pp. 2108-2115.
[21] Fayala, I., O. Limam, and I. Stefanou. 2016. “Experimental and numerical analysis of reinforced stone block masonry beams using GFRP reinforcement”. *Composite Structures*, 152: 994-1006.
[22] Derakhshan, H., et al. 2014. “In situ out-of-plane testing of as-built and retrofitted unreinforced masonry walls”. *Journal of Structural Engineering*, 140(6): 04014022.
[23] Boscato, G., et al. 2014. “Seismic Behavior of a Complex Historical Church in L'Aquila”. *International Journal of Architectural Heritage*, 8(5): 718-757.
[24] Casapulla, C. and L.U. Argiento. 2016. “The comparative role of friction in local out-of-plane mechanisms of masonry buildings. Pushover analysis and experimental investigation”. *Engineering Structures*, 126: 158-173.

Highlights

- The paper presents a preliminary simplified procedure to evaluate the seismic safety of masonry buildings retrofitted with reinforced concrete roofs.
- Effective connection between RC roof and walls is crucial to be in a safe condition
- Sensitivity analyses performed to evaluate the influence of each input parameter
- In most cases nonlinear kinematic analyses provide larger safety factors

The role of reinforced concrete roofs in the seismic performance of masonry buildings

Alessandro Cardoni[a], Gian Paolo Cimellaro[b,*]

[a]PhD Student, Department of Structural, Geotechnical and Building Engineering, Politecnico di Torino, Corso Duca degli Abruzzi 24, 10129, Turin, Italy. E-mail: alessandro.cardoni@polito.it

[b]Associate Professor, Department of Structural, Geotechnical and Building Engineering, Politecnico di Torino, Corso Duca degli Abruzzi 24, 10129, Turin, Italy. E-mail: gianpaolo.cimellaro@polito.it

[*]Corresponding author. Tel.: +39 011 0904801. E-mail: gianpaolo.cimellaro@polito.it

Abstract

The 2016 Central Italy earthquake caused many collapses of existing masonry buildings that had previously been retrofitted with reinforced concrete roofs. The aim of this paper is to explore the role of these roofs in the seismic behaviour of masonry buildings. Simple analytical models are presented to illustrate two typical out-of-plane collapse mechanisms: wall overturning and vertical flexure. The models are based on linear kinematic analysis, which allows fast modelling and calculation of a coefficient that can be used to assess the safety level of a structure. Nonlinear kinematic analyses were also performed. Both methods were applied to two case studies taken from areas struck by the earthquake. Results show that linear analysis represents an effective tool for preliminary verifications that can allow one to understand whether retrofit interventions are needed.

Keywords: masonry, reinforced concrete roof, collapse, retrofit, kinematic analysis, Central Italy earthquake

1. Introduction

After the 24th August 2016 Central Italy earthquake, most of the buildings of small towns nearby the epicenter were declared unsafe and several structures collapsed completely. Poor material quality and scant building techniques were certainly the main reason of collapses. However, inadequate retrofit interventions also contributed to the disruptive effect of the seismic event. For instance, the replacement of the old wooden roofs with reinforced concrete roofs seemed to facilitate some mechanisms that led to severe damages and collapses. This type of retrofitting was broadly adopted in the 80s and 90s since it was believed to be effective against seismic actions. In fact, it was the Italian code itself to recommend it [1] . Moreover, at that period there was a massive use of concrete that led to a gradual abandon of research and experimental tests on masonry [2] . The overall idea was to put robust structures such as RC roofs and floors connected to perimetric walls by means of RC ring beams to avoid independent movements of masonry macro-elements. After Tolmezzo earthquake in 1976, this and other retrofitting techniques became part of technical codes, until Umbria and Marche earthquake in 1997 [3, 4] .

This event pointed out the disadvantages of heavy and stiff roofs and floors. In fact, if vertical structures are not robust enough, they are indeed the primary cause of collapses. The significant stiffness and load increment at the top have led to the collapse of the walls, which were made of poor materials and not strengthened. Conversely, there were also many cases of masonry structures retrofitted with reinforced concrete roofs that withstood the earthquake with no significant damages (Figure 1).

Figure 1. Masonry buildings retrofitted with concrete roof not collapsed after the earthquake in Pescara del Tronto (a-b) and small villages near Accumoli (c-d).

However, there is no guarantee that those buildings are safe. Therefore, in this paper a simple verification procedure that is able to estimate the level of safety of masonry buildings with reinforced concrete roofs is implemented. The adopted approach is based on the linear kinematic analysis, which is also described by Italian codes [5, 6]. Despite the method is well known in its theoretical formulation, it is rarely used and usually the effect of the roof and the connection among structural elements are neglected. This research contributes to the current literature with practical applications of the kinematic analysis introducing simplified analytical models that take into account the effect of reinforced concrete roofs. An additional advantage of the proposed models is that the number of input parameters has been reduced as much as possible so that the analysis does not require any particular investigation or survey to be carried out. A safety factor was also defined to assess the safety level of the building towards different collapse

mechanisms. The choice of a simplified procedure has been made in order to have a fast tool which could be used even by non-professional users. The method would allow property owners to understand if they are in danger. For instance, if the obtained safety factor is low or close to the unsafe threshold, further investigations should be conducted. More detailed methods have been studied by many authors to describe masonry buildings behaviour, but they need to be calibrated and the input data are often not accessible [7-10]. Obviously, results will not be as accurate, and a certain margin of error should be taken into account in final considerations. Nonetheless, they can provide relevant preliminary information about the structure. In addition, in the literature there is a number of studies about masonry where analytical models turned out to be highly effective and close to the real behaviour [11, 12].

After defining the formulation, the method is applied to different models describing the overturning and the vertical flexural behaviour. The models derive from those commonly used to study the out-of-plane mechanisms [13-15] and the arch rocking [16-18]. To analyse the influence of the connection between the roof and the floor to the walls, a ring beam is also considered. The presence of a reinforced concrete (RC) ring beam is dangerous if it is not well connected to masonry walls and if the latter is not strengthened. Furthermore, the spread of reinforced concrete in the construction sector, led to wrong applications in the interventions of existing buildings. Nowadays there are many solutions to realize effective structural connections, such as reinforced masonry ring beams [19]. The use of innovative composite materials has become a common practice in retrofit strategies. Several studies have been carried out in this field which has allowed to investigate the behavior of strengthened beams [20, 21] and strengthened masonry walls through out-of-plane tests [22].

Two case studies taken from two towns struck by the abovementioned earthquake were analyzed, but the method can be extended to any building by choosing appropriate parameters. Both examples were selected by considering typical houses in the area, built with local materials and poor construction techniques and retrofitted with reinforced concrete roofs. The first one is 1-storey building while the second one has two storeys and thus also the action of the inter-storey floor is considered in the model. For each model, the linear kinematic analysis is repeated for different values of the input parameters, as they could be affected by uncertainty. In this way it is possible to see the influence of a single parameter and what happens if it is over-estimated or under-estimated. Finally, nonlinear analyses are performed in order to compare the results and understand if the additional computational effort of a more refined method is worth it.

2. The linear kinematic analysis

In existing masonry buildings there are often collapses due to a loss of equilibrium of some portions of bearing structures. In general, these types of mechanisms happen when seismic forces act in the out-of-plane direction. The linear kinematic analysis can be used to study these phenomena and for the verification process. It is based on the choice of the possible mechanisms that are most likely to happen. These ones are assumed by evaluating the current cracking state and analyses performed on similar buildings. In the literature there are plenty of studies on historical buildings, such as churches, which are helpful to clarify how the collapse process activates and evolve [23]. The ability to detect the most probable mechanisms is crucial to prevent local or global collapses, since it is possible to run specific analyses and consequently suggest specific interventions.

The linear kinematic approach schematizes the building in a discrete number of macro-elements which move according to their boundary conditions. For this reason, the assumptions are that the material has no tensile strength and infinite compressive strength. In each rigid block, vertical loads (including dead and external loads) and a system of horizontal forces are applied. Horizontal forces are proportional to the vertical loads through a coefficient called load multiplier (α). Incrementing the load multiplier, it is possible to evaluate the horizontal force that activates a specific mechanism. α_C is named the collapse load multiplier, and it is calculated with the principle of virtual works. Therefore, the total work of the external forces (L_e) has to be equal to the total work of the internal forces (L_i) which in this case is null as shown in Eq. (1):

$$L_e = \alpha_C \left(\sum_{i=1}^{n} W_i \cdot \delta_{x,i} + \sum_{j=n+1}^{n+m} W_j \cdot \delta_{x,j} \right) - \sum_{i=1}^{n} W_i \cdot \delta_{y,i} - \sum_{h=1}^{o} F_h \cdot \delta_h = L_i = 0 \quad (1)$$

where: n is the number of the weight forces applied to all macro-elements; m is the number of weight forces that generate horizontal forces upon macro-elements; o is the number of external forces; W_i is the generic weight force; W_j is the generic weight force that generates horizontal forces upon macro-elements; $\delta_{x,i}$ is the virtual horizontal displacement of the point where the i-th weight force is applied; $\delta_{y,i}$ is the virtual vertical displacement of the point where the i-th weight force is applied; F_h is the generic external force; δ_h is the virtual displacement of the point where the generic external force F_h is applied. Eq. (1) often becomes an equilibrium equation between a stabilizing moment and an overturning moment, so it is not necessary to calculate the virtual displacement. The method is also used to determine the most probable collapse mechanism which is the one that requires less energy to be activated (i.e. the one with the lower load multiplier). However, the decay conditions of masonry should never be neglected since they are able to reveal if a specific mechanism has already been activated. Once α_C is calculated, it is possible to obtain the acceleration that generates the mechanism (Eq. (2)).

$$a_0^* = \frac{\alpha_C \cdot \sum_{i=1}^{n+m} P_i}{M^* \cdot FC} \quad (2)$$

where FC is a coefficient that depends on the level of knowledge about the masonry structure. The level of knowledge is based on information like geometry, construction details, and material properties. Such data can be acquired in different ways, from generic research and visual inspection to extensive tests and measurements. Since the material strength is not considered in this research, only basic information about geometric characteristics, type of masonry panels and construction details was collected. According to the Italian code [6], three level of knowledge can be identified: limited, extended and exhaustive. Due to the limited available data, the level of knowledge is limited. In this case, the code reports the FC coefficient has to be assumed equal to 1,35 which reduces the acceleration that generates the mechanism. M^* is the participating mass, calculated considering the virtual displacements of the points where the loads are applied, as shown in Eq. (3) [6]:

$$M^* = \frac{\left(\sum_{i=1}^{n+m} P_i \cdot \delta_{x,i}\right)^2}{g \cdot \sum_{i=1}^{n+m} P_i \cdot \delta_{x,i}^2} \quad (3)$$

The acceleration given by Eq. (2) has now to be compared with an allowable acceleration. This one is given by Eq. (4), which is valid when the analysed blocks are in contact with the ground, meaning that the mechanism involves ground floor walls:

$$a^* = \frac{a_g \cdot S}{q} \quad (4)$$

where: a_g is the peak ground acceleration at the site determined, as indicated by Italian codes, for a return period of 475 years; q is the reduction factor which can be assumed equal to 2 for regular masonry structures; S is given by the product of two coefficients: S_s that depends on the soil category and represents the stratigraphic amplification, and S_t which takes into account the effects of the topographical amplification and depends on the surface configuration of the soil.

It is clear that the acceleration that activates the mechanism should be greater than the allowable one. To quickly verify this, it is possible to introduce a safety factor which is the ratio between the two accelerations (Eq. (5)):

$$SF = \frac{a_0^*}{a^*} \geq 1 \quad (5)$$

3. Analytical models

In some cases, there are mechanisms that are suggested by the building itself just looking to the geometry, the nature of the structural elements, the cracking state, the interventions occurred over the years, etc. The linear kinematic analysis is a powerful tool that can be used to describe local mechanisms that have been observed after disruptive earthquakes. If only out-of-plane mechanisms are considered, then they can be basically grouped in three categories: (i) overturning, (ii) vertical flexural behaviour and (iii) horizontal flexural behaviour. In this paper only the first two categories are considered since they were the main cause of collapses during the Central Italy earthquake. In addition, for these two mechanisms the presence of a reinforced concrete roof is more crucial. For the overturning, two cases were studied, a 1-storey and a 2-storey building, whereas for the vertical flexural behaviour only the 2-storey building was studied, taking into account also the effect of the inter-storey. The considered macro-elements are the walls, the floor, and the reinforced concrete roof. This one is assumed as an element that transfers only vertical loads to the walls and no lateral thrusts. Therefore, it is modelled as a rigid block with a large mass. The effects of perpendicular walls are neglected, as in many real cases there are no connections. All models consider alternatively the presence and the absence of connections between roof and walls (by means of a ring beam) and between floor and walls. When there is a ring beam the roof is fixed to the walls and moves with them, while when there is no connection the roof is considered simply supported.

3.1 1-storey overturning without ring beam

This is the case of simple overturning where there is no ring beam, and therefore no connection between the top of the wall and the roof. For this reason, the macro-elements are independent one from another and only one wall is subjected to overturning. Figure 2 illustrates the mechanism and the forces involved. W_1 is the weight of the left wall, P_R is the weight of the roof applied in its center of mass G_R and split equally between the two walls.

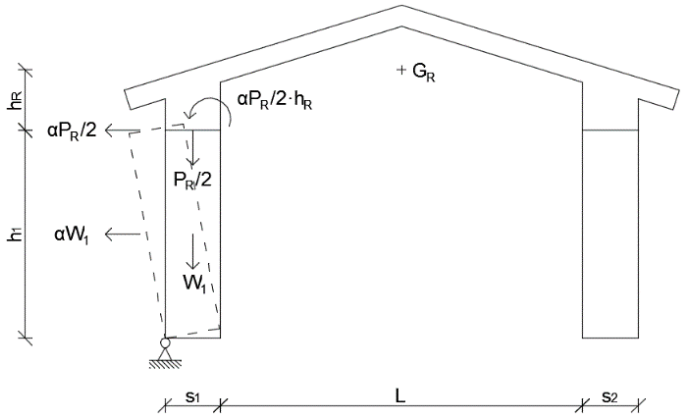

Figure 2. Calculating scheme for 1-storey overturning without ring beam.

According to Eq. (1) the load multiplier that leads to collapse for this configuration is given by Eq. (6):

$$\alpha_C = \frac{W_1 \cdot \frac{s_1}{2} + \frac{P_R}{2} \cdot \frac{s_1}{2}}{W_1 \cdot \frac{h_1}{2} + \frac{P_R}{2} \cdot \left(h_1 + h_R\right)} \tag{6}$$

where s_1 is the thickness of left wall; h_1 is the height of walls; h_R is the distance between the top of walls and the center of mass (G_R) of the roof, and L is the span length.

3.2 1-storey overturning with ring beam

If there is a ring beam the two external walls are connected at the top to realize the so called "box-like" behaviour. Macro-elements are no more independent, so they move together until the loss of equilibrium. As shown in Figure 3 both walls rotate around the hinge at the bottom under a seismic action. The effect of the ring beam is modelled using a force acting in the opposite direction of the kinematic movement. To a first approximation, it can be calculated as the product of the friction coefficient μ and the weight of the roof P_R. For the estimation of the friction coefficient there are many experimental tests available in literature [24]. However, since the proposed model is simplified and no detailed information about the materials were available, the guidelines provided by national codes were followed [5, 6]. In particular, as a precautionary measure, a friction coefficient of 0.4 was used, which is the lowest among the suggested values.

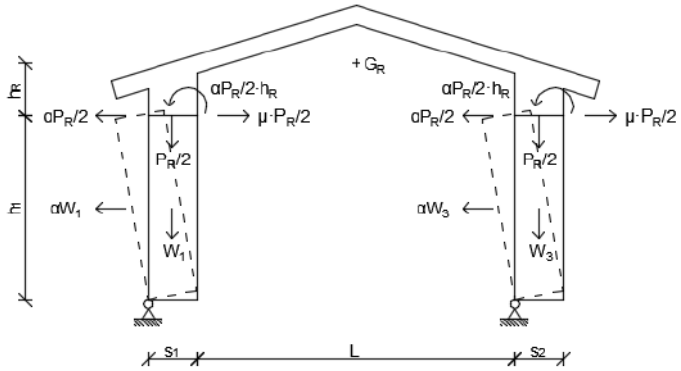

Figure 3. Calculating scheme for 1-storey overturning with ring beam.

Eq. (7) gives the collapse load multiplier in the case of overturning with ring beam:

$$\alpha_C = \frac{\left(W_1 + \frac{P_R}{2}\right)\cdot\frac{s_1}{2} + \left(W_3 + \frac{P_R}{2}\right)\cdot\frac{s_2}{2} + \left(\mu\cdot P_R\right)\cdot h_1}{\left(W_1 + W_3\right)\cdot\frac{h_1}{2} + P_R\cdot\left(h_1 + h_R\right)} \tag{7}$$

where s_1, s_2 are the thicknesses of left and right walls, respectively; W_1 is the weight of the left wall, while W_3 is the weight of the right one.

3.3 2-storey overturning without ring beam

This model is an extension of the 1-storey model, so the same assumptions can be made. However, in this model there is a new macro-element, the floor of weight P_F that is split equally between the left and the right wall. In a simplified manner, in the current model and the ones below, the contact area between the inter-storey floor and ground floor walls is assumed to be half the thickness of walls. To allow a complete rotation of the two masonry panels, the floor is considered disconnected to the walls and the connection to the ground is modelled as a hinge (Figure 4). The formulation of the load multiplier α_C is given by Eq. (8):

$$\alpha_C = \frac{\left(W_1 + W_2 + \frac{P_R}{2}\right)\cdot\frac{s_1}{2} + \frac{P_F}{2}\cdot\frac{3s_1}{4}}{W_1\cdot\frac{h_1}{2} + \frac{P_F}{2}\cdot h_1 + W_2\cdot\left(h_1 + \frac{h_2}{2}\right) + \frac{P_R}{2}\cdot\left(h_1 + h_2\right) + \frac{P_R}{2}\cdot h_R} \tag{8}$$

where W_2 is the weight of the left masonry panel of the upper level and h_2 is its height.

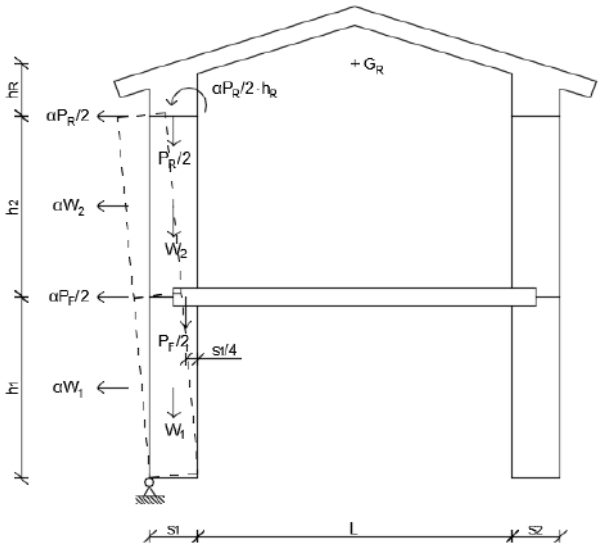

Figure 4. Calculating scheme for 2-storey overturning without ring beam.

3.4 2-storey overturning with ring beam

As already seen in the 1-storey case, the ring beam at the roof level connects the walls together, so they can overturn at the same time. Once again, the connection is modelled as a friction force proportional to the weight of the roof (Figure 5). In this case, the inter-storey floor is well connected to the walls and moves together with them. Eq. (9) provides the collapse load multiplier for this case:

$$\alpha_C = \frac{\left(W_1 + W_2 + \frac{P_R}{2}\right)\cdot\frac{s_1}{2} + \frac{P_F}{2}\cdot\frac{3s_1}{4} + \left(W_3 + W_4 + \frac{P_R}{2}\right)\cdot\frac{s_2}{2} + \frac{P_F}{2}\cdot\frac{s_2}{4} + (\mu\cdot P_R)\cdot(h_1 + h_2)}{(W_1 + W_3)\cdot\frac{h_1}{2} + P_F\cdot h_1 + (W_2 + W_4)\cdot\left(h_1 + \frac{h_2}{2}\right) + P_R\cdot(h_1 + h_2) + P_R\cdot h_R} \quad (9)$$

where W_4 is the weight of the right masonry panel of the upper level.

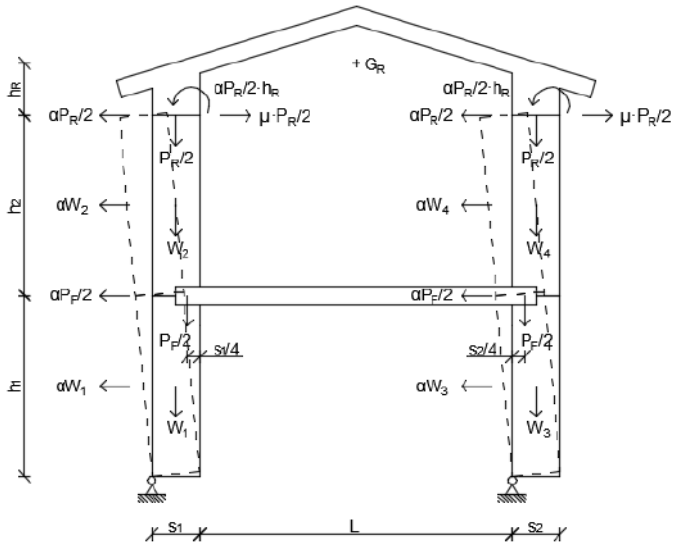

Figure 5. Calculating scheme for 2-storey overturning with ring beam.

3.5 2-storey flexural behaviour without connection between floor and walls

Vertical flexural behaviour can occur in any part of the wall. It can be seen as a triple-hinged arch where, in this specific case, the hinges are located at the bottom, at the top, and at the inter-storey level. This means that the mechanism is activated by the horizontal inertial force caused by the floor during the seismic action. The upper level wall is connected at the top of the roof, whereas the inter-storey floor is not connected to the walls (Figure 6). The collapse load multiplier α_C is given by Eq. (10):

$$\alpha_C = \frac{W_1 \cdot \frac{s_1}{2} + W_2 \cdot \left(s_1 + \frac{s_1}{2} \cdot \frac{h_1}{h_2} \right) + \frac{P_F}{2} \cdot \frac{3s_1}{4} + \frac{P_R}{2} \cdot \left(s_1 + \frac{s_1}{2} \cdot \frac{h_1}{h_2} \right)}{W_1 \cdot \frac{h_1}{2} + W_2 \cdot \left(h_1 \cdot \frac{h_1}{h_2} + \frac{h_2}{2} \cdot \frac{h_1}{h_2} \right) + \frac{P_F}{2} \cdot h_1} \tag{10}$$

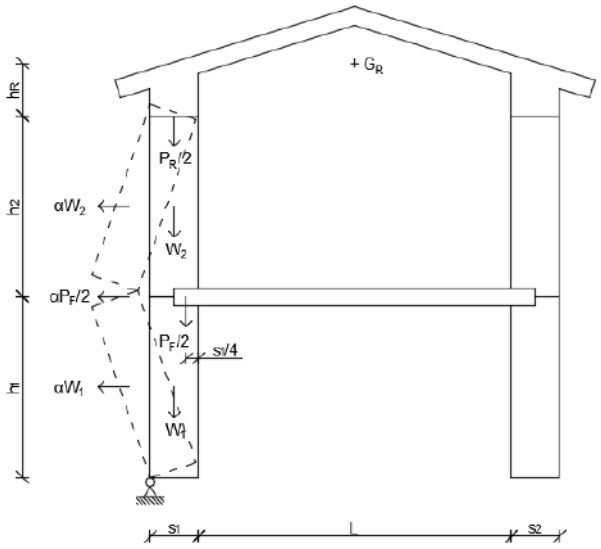

Figure 6. Calculating scheme for vertical flexural behaviour without floor-walls connection.

3.6 2-storey flexural behaviour with connection between floor and walls

In this model the floor is well connected to the walls so that it can pull them together, but eventually it detaches. To represent this type of connection, a friction force proportional to the floor weight is considered at the inter-storey level (Figure 7).

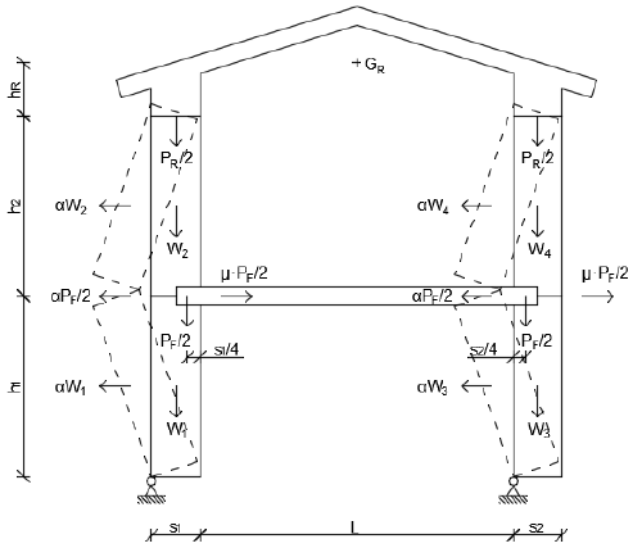

Figure 7. Calculating scheme for vertical flexural behaviour with floor-walls connection.

Eq. (11) allows to get the collapse load multiplier for this model:

$$\alpha_C = \frac{W_1 \cdot \frac{s_1}{2} + W_2 \cdot \left(s_1 + \frac{s_1}{2} \cdot \frac{h_1}{h_2} \right) + W_3 \cdot \frac{s_2}{2} + W_4 \cdot \left(s_2 + \frac{s_2}{2} \cdot \frac{h_1}{h_2} \right) + \frac{P_F}{2} \cdot \frac{3s_1}{4} + \frac{P_F}{2} \cdot \frac{s_2}{4}}{\left(W_1 + W_3 \right) \cdot \frac{h_1}{2} + \left(W_2 + W_4 \right) \cdot \left(h_1 \cdot \frac{h_1}{h_2} + \frac{h_2}{2} \cdot \frac{h_1}{h_2} \right) + P_F \cdot h_1} + \frac{\frac{P_R}{2} \cdot \left(s_1 + \frac{s_1}{2} \cdot \frac{h_1}{h_2} \right) + \frac{P_R}{2} \cdot \left(s_2 + \frac{s_2}{2} \cdot \frac{h_1}{h_2} \right) + \left(\mu \cdot P_F \right) \cdot h_1}{\left(W_1 + W_3 \right) \cdot \frac{h_1}{2} + \left(W_2 + W_4 \right) \cdot \left(h_1 \cdot \frac{h_1}{h_2} + \frac{h_2}{2} \cdot \frac{h_1}{h_2} \right) + P_F \cdot h} \tag{11}$$

4. Case studies

4.1 Pescara del Tronto case study

Figure 8 shows a house in Pescara del Tronto completely collapsed after the 2016 Central Italy earthquake, which can be used as an example to apply the 1-storey model. The data that were used as input in the model are the following: wall thickness ($s = s_1 = s_2$) = 0.4 m; roof thickness (s_R) = 0.15 m; wall height (h_1) = 3 m; wall length (l_w) = 7 m; span length (L) = 5 m; distance between the center of mass of the roof and the top of the wall (h_R) = 0.4 m; specific weight of masonry (P_m) = 19 kN/m^3; specific weight of reinforced concrete (P_c) = 21 kN/m^3; friction coefficient roof – wall (μ) = 0.4; PGA for a return period of 475 years (a_g) = 2.489 m/s^2; S_s = 1 (rock soil); S_t = 1.2 (top of a hill). The weight of the walls was calculated as $W_i = h_i \cdot l_w \cdot s_i \cdot P_m$, where $i=1, 2$, while the weight of the roof as

$$W_i = 2 \cdot \left[\sqrt{\left(s + L/2 \right)^2 + h_r^{\,2}} \cdot l_w \cdot s_r \cdot P_c \right].$$

Figure 8. View of the building used as case study before and after the earthquake.

As already mentioned, most of the data are geometrical so they can be easily collected. Only the PGA needs to be calculated referring to the information given by the Italian code [5]. In this case, the location is fixed, so the value can be determined analytically. The value used for S_s is referred to rock soil, while the one used for S_t is referred to the top of a hill as there is evidence of a slope behind the building.

4.1.1 Pescara del Tronto results

The results using the linear kinematic analysis and verification are reported in Table 1.

Table 1. Collapse load multipliers and safety factors for the Pescara del Tronto case study.

	1-storey overturning without ring beam	1-storey overturning with ring beam
α_C	0.10	0.26
SF	0.57	1.48

Comparing the load multipliers, it can be observed that the first mechanism is more likely to happen as the 1-storey overturning with ring beam case has a collapse load 2.6 times higher than the 1-storey overturning without ring beam. This is confirmed by the fact that the safety factor in the case without ring beam is lower and it is below the safety threshold. Indeed, as shown in Figure 8 there is no connection between roof and walls. If this kind of analysis was carried out in a pre-earthquake situation, it would have been possible to demonstrate how the building was unsafe towards a seismic event with a return period of 475 years. The actual demand of 2016 earthquake was larger than the one used as input for this verification procedure. However, the aim of the method is to report if retrofitting is needed to improve the level of safety. Validation analyses were not performed at this stage, but adequate interventions could have likely prevented the structure from a complete collapse.

A sensitivity analysis was carried out to assess the impact of the chosen input parameters on results. Most relevant outcomes were then plotted in graphs with the varying parameter on the *x* axis and the safety factor *SF* on the *y* axis. Figure 9(a) shows that when there is no

friction the two mechanisms are equivalent because of the symmetry of the systems and the configuration is unsafe. The minimum friction coefficient to ensure a safety factor greater than 1 is 0.2. As predictable, the impact of the friction is overall positive: it is enough to build a ring beam able to ensure a friction coefficient of 0.4 and triple the safety factor. In Figure 9(b) the span length is varying, resulting in an increase or decrease in the weight of the roof. This has almost no effects in the case without ring beam, which remains unsafe in the whole range of variation. On the other hand, since the friction force is proportional to the weight of the roof, increasing the span length leads to a significant increment of the safety factor. When the masonry specific weight of the masonry varies, safety factor remains almost constant (Figure 9(c)). The weight of the walls has indeed a twofold effect since it contributes to both stabilizing and overturning forces. Also, looking at the equations that lead to determine SF (in particular Eqs. (6-7) and Eq. (2)), it can be noticed how the weight appears always at both nominator and denominator. Therefore, in the calculation steps its variation tends to have negligible effects. Figure 9(d) shows the influence of the wall thickness. In the first case, without ring beam, an increment of the wall thickness corresponds to a linear and considerable increment of the *SF*. However, almost 70 cm walls are required to be in the safe area. In the second case, there is an asymptotic trend. It means that for low thicknesses the presence of the ring beam is effective (e.g. for s = 20 cm the *SF* is two times the *SF* in the case with no ring beam), but for high thicknesses the structure is so massive that the presence of the ring beam at the top is irrelevant. Finally, in Figure 9(e) different soil categories are taken into account by varying the abovementioned parameter S_s. Following the guidelines provided by the Italian seismic codes, the possible values S_s can assume were calculated (Table 2). A rock soil allows to have higher safety factors, whereas if the quality gets worse there is a decreasing trend, except for category E (coarse soil upon a stiff or soft soil).

Table 2. Values of the parameter S_s for different soil categories.

Soil category	**Description**	S_s
A	Rock soil (Vs30 > 800 m/s)	1.00
B	Soft rock and very dense soil (360 m/s < Vs30 < 800 m/s)	1.16
C	Stiff soil (180 m/s < Vs30 < 360 m/s)	1.33
D	Soft soil (Vs30 < 180 m/s)	1.48
E	Coarse soil upon stiff or soft soil	1.33

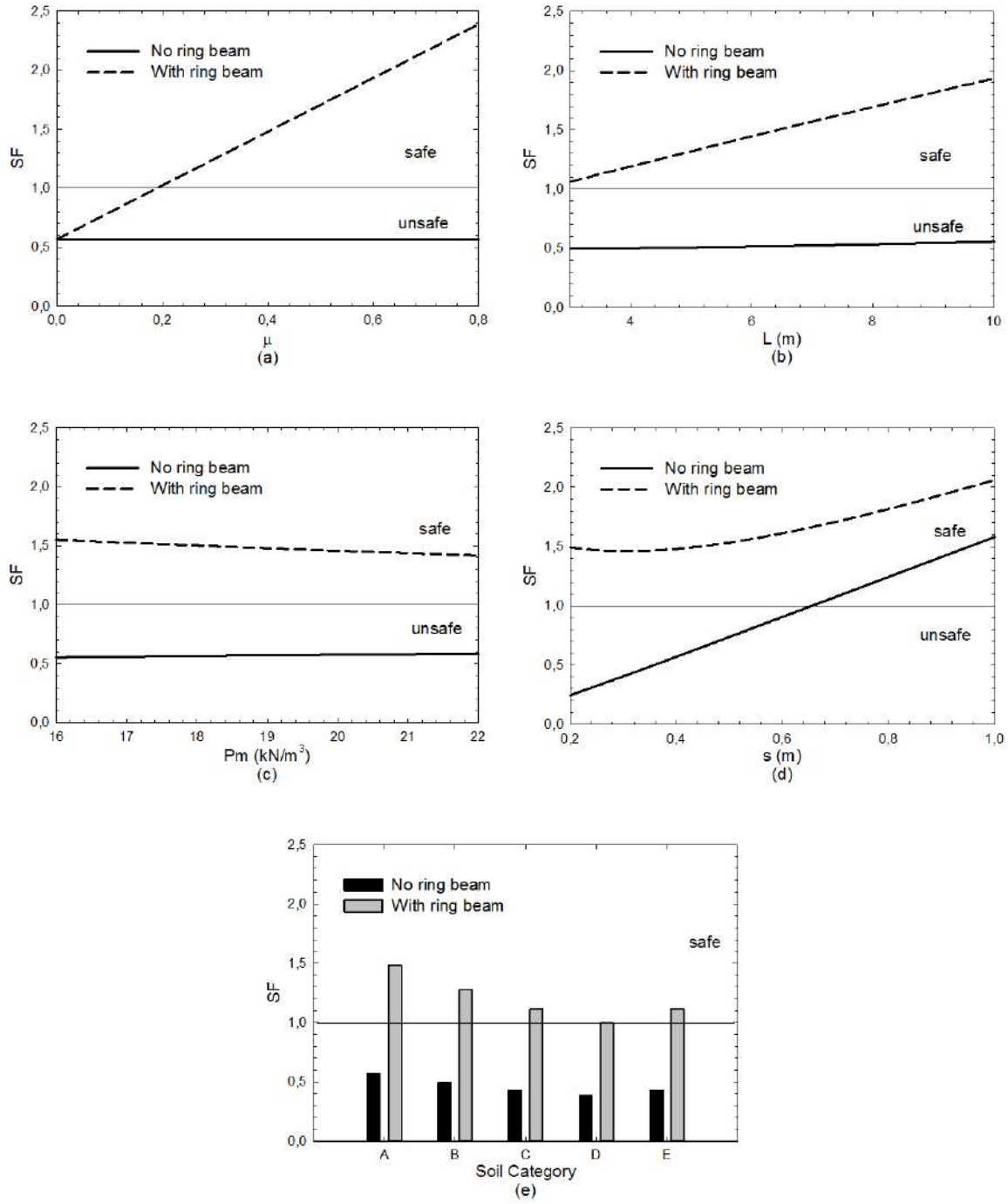

Figure 9. (a) Friction coefficient vs. safety factor, (b) span length vs. safety factor, (c) masonry specific weight vs. safety factor, (d) wall thickness vs. safety factor, (e) soil category vs. safety factor.

4.2 Amatrice case study

The 2-floor models were tested through the building in Figure 10 which was located in Amatrice. The data used as input for the analysis are the following: wall thickness ($s_1 = s_2$): 0.4 m; roof thickness (s_R): 0.15 m; wall height ($h_1 = h_2$): 3 m; wall length (l_w): 11 m; span length (L): 6.5 m; distance between the center of mass of the roof and the top of the wall (h_R):

0.4 m; specific weight of the masonry (P_m): 19 kN/m^3; specific weight of the reinforced concrete (P_c): 21 kN/m^3; floor weight (P_f): 4 kN/m^2; friction coefficient roof – wall (μ): 0.4; friction coefficient floor – wall (μ): 0.5; PGA for a return period of 475 years (a_g): 2.538 m/s^2; S_s: 1 (rock soil); S_t: 1 (flat area).

Figure 10. View of the building used as case study before and after the earthquake.

4.2.1 Amatrice results

The results obtained using the linear kinematic analysis are summarized in Table 3:

Table 3. Collapse load multipliers and safety factors for the Amatrice case study.

	2-storey overturning without ring beam	2-storey overturning with ring beam	2-storey vertical flexural behaviour without connection between floor and walls	2-storey vertical flexural behaviour with connection between floor and walls
α_C	0.06	0.16	0.16	0.27
SF	0.44	1.14	1.03	1.70

Comparing these results, it is clear that the configuration of overturning with no ring beam is the less safe and the most probable. The presence of a ring beam increases the collapse load multiplier of about 2.7 times for the overturning mechanism. On the other hand, the model with connection at the top of the walls and at floor level is the safest and less probable case. For the vertical flexural behaviour, the case with connection between floor and walls has 1.7 times as high of a collapse load as the case without connection has. Finally, it is possible to observe that the mechanisms of overturning with ring beam and vertical flexural behaviour without connection at floor level are almost equivalent.

Also for this case study, sensitivity analyses were performed for all parameters. The trends of variation of other parameters are really similar to the previous ones, thus the considerations done for the 1-storey model are still valid. The substantial difference between 2-storey overturning and vertical flexural behaviour is that in the second case the safety factors are higher. Omitting obvious and well-known results, it is worth to comment what happens when the floor weight is changing (Figure 11). In both cases of overturning and in the case of

vertical flexural behaviour without connection, when the floor weight varies the safety factor is not subject to significant changes. A slight reduction of SF can be observed in the overturning scenario for the model with ring beam as the floor weight increases. A heavier floor leads to greater horizontal inertial forces which contribute to the overturning. Instead, for the mechanism of vertical flexural behaviour with connection, a heavy floor has a positive impact since the stabilizing force increases. As far as the variation of soil category is concerned, the values of the S_s coefficient that were used in the previous case study are still valid (Table 2). It is interesting to notice that if the category of soil was not "A" (rock soil), then only the mechanism of vertical flexural behaviour with connection would be safe (Figure 12).

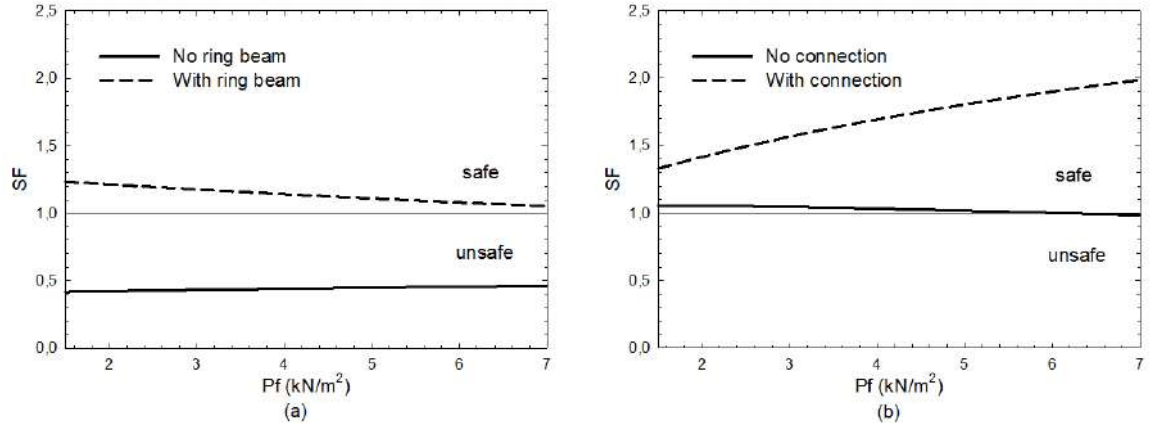

Figure 11. Floor weight vs. safety factor for the (a) overturning mechanism and the (b) vertical flexural behaviour.

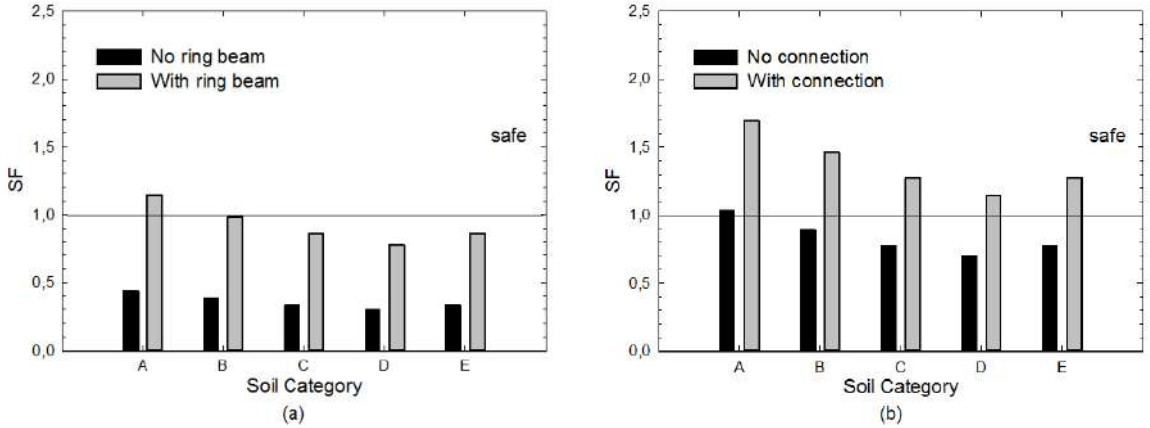

Figure 12. Soil category vs. safety factor for the (a) overturning mechanism and the (b) vertical flexural behaviour mechanism.

5. Nonlinear kinematic analysis

Nonlinear kinematic analyses were carried out with the aim of supporting the results obtained from linear analyses. The whole procedure follows the method proposed by Italian codes [5,

6], which is presented hereafter just in its main steps. The underlying idea of the method is to determine the trend of the horizontal action that the structure is progressively able to withstand during the collapse mechanism's evolution. This can be seen as the capacity curve of an equivalent single degree of freedom system. The ultimate displacement capacity of the local mechanism is then defined and compared with the seismic demand. Similarly to the linear case, a multiplier α is introduced and defined as the ratio between the applied horizontal forces and the displacement d_k of a control point. The horizontal multiplier of loads is evaluated at various configurations of the kinematic chain until reaching the collapse condition, which is identified by a null multiplier α, and a displacement $d_{k,0}$. Assuming that involved actions (i.e. weights, external and internal forces) are constant during the evolution of the mechanism, the curve is almost linear. In this case, only the evaluation of the displacement $d_{k,0}$ is required, and the curve is described by Eq. (12):

$$\alpha = \alpha_0 (1 - d_k / d_{k,0}) \tag{12}$$

where α_0 denotes the value of the multiplier capable of activating the analysed mechanism. The problem can be solved considering a configuration varied from the static condition and calculating the induced finite rotation θ_k by means of virtual work principle. Reaching the collapse situation, the overturning moment equals the stabilizing moment, and the resulting nonlinear equation gives the final rotation $\theta_{k,0}$. Once the latter is determined, the corresponding displacement $d_{k,0}$ can be obtained. Let the control point be the center of gravity of vertical forces, and h_{bar} be its distance from the base hinge. Eq. (13) expresses the relation between the rotation angle and the displacement of the control point related to ultimate capacity towards horizontal actions.

$$d_{k,0} = h_{bar} sin\theta_{k,0} \tag{13}$$

At this point, it is possible to define the α - d_k curve according to Eq. (12). The equivalent capacity curve should now be determined. It describes the relation between the acceleration a^* that activates the mechanism and displacement d^*. The first is obtained through Eq. (2) as in the linear case, whereas d^* is given by Eq. (14).

$$d^* = d_{k,0} \frac{\sum_{i=1}^{n+m} P_i \delta_{x,i}^2}{\delta_{x,k} \sum_{i=1}^{n+m} P_i \delta_{x,i}} \tag{14}$$

where: $n+m$ is the number of weight forces that generates horizontal forces upon the macro-elements; P_i is the generic weight force; $\delta_{x,i}$ is the virtual horizontal displacement of the application point of P_i; $\delta_{x,k}$ is the horizontal virtual displacement of the control point.

Making the same assumption done for the α - d_k curve, the capacity curve can be derived from Eq. (15).

$$a^* = a_0^* (1 - d^* / d_0^*) \tag{15}$$

where d_0^* is the equivalent displacement corresponding to $d_{k,0}$.

The verification for the life safety limit state consists in a comparison between the ultimate displacement capacity d_u^* of the local mechanism and the spectral displacement evaluated at the period T_s (Eq. (16)):

$$T_s = 2\pi\sqrt{\frac{d_s^*}{a_s^*}} \tag{16}$$

where a_s^*, is the acceleration correspondent to the displacement d_s^*, which is equal to $0.4d_u^*$, and $d_u^* = 0.4d_0^*$. Therefore, if d_u^* is greater than the spectral displacement $S_{De}(T_s)$, the verification is fulfilled (Eq. (17)).

$$SF = \frac{d_u^*}{S_{De}(T_s)} \geq 1 \tag{17}$$

Table 4 shows obtained results for all analysed models. As expected, a lack of connection is responsible of a small safety factor, always around 1 for the three studied cases. On the other hand, the presence of a ring beam or floor-wall connections ensures much more capacity to withstand larger ultimate displacements, which also means a higher safety level. The difference is less exaggerated in the case of vertical flexural behaviour since the connection between the floor and the wall makes the structure more rigid.

Comparing the linear with the nonlinear kinematic analysis in terms of safety factors, the bar chart of Figure 13 can be plotted. The nonlinear kinematic analysis usually provides safety coefficients that are two times or more the coefficient obtained with the linear analysis. This confirms that a fast and preliminary analysis, such as the linear one, provides precautionary results and it is recommended to understand if further investigations are needed. The described trend is inverted in the cases of vertical flexural behaviour, although the nonlinear safety factors are just slightly lower than linear ones. This phenomenon is due to the fact that the weight of a reinforced concrete roof has a particularly positive effect for these two models. In addition, the same analyses were repeated several times increasing the weight of the roof for each iteration. In all cases the safety factor increased, but the increment in the linear analysis was greater than in the nonlinear one.

Table 4. Results of the nonlinear kinematic analysis.

	Pescara del Tronto		**Amatrice**			
	1-storey overturning without ring beam	**1-storey overturning with ring beam**	**2-storey overturning without ring beam**	**2-storey overturning with ring beam**	**2-storey flexural behaviour without connection**	**2-storey flexural behaviour with connection**
d_u^* **[m]**	0.089	0.227	0.093	0.326	0.041	0.074
SF	1.04	2.66	1.02	3.02	1.12	1.95

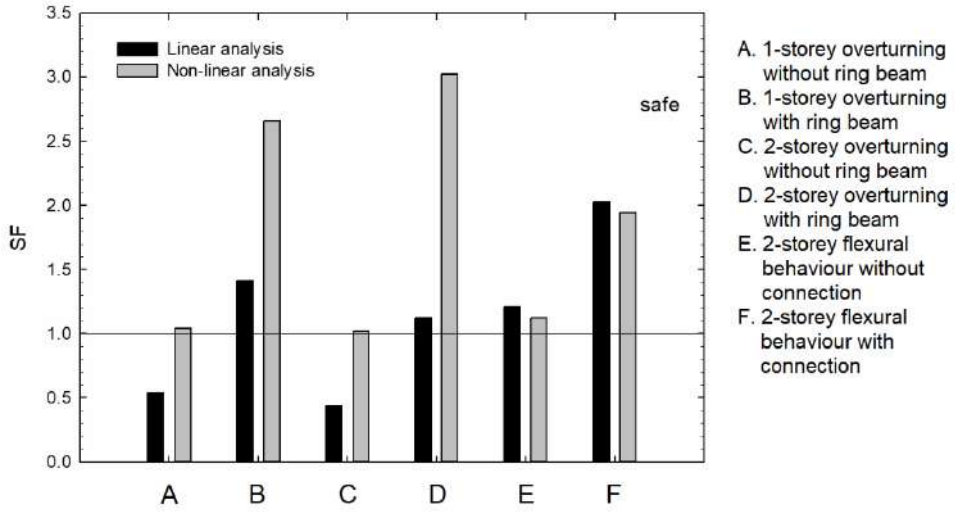

Figure 13. Comparison between safety factors resulting from linear and non-linear analyses.

6. Conclusions

The 2016 Central Italy earthquake caused damages and collapses of many masonry buildings, including those retrofitted with reinforced concrete roofs. This type of retrofit intervention seems to facilitate some collapse mechanisms if not properly executed. The paper presents a simplified procedure to evaluate the seismic performance of masonry buildings retrofitted with reinforced concrete roofs based on the linear kinematic analysis. Despite the analysis method is well known, the proposed models have the advantage of explicitly considering the interaction between the roof and the walls. Moreover, they require only few input parameters that can be easily obtainable. The collapse load multiplier obtained as output of the linear kinematic analysis was used to define a safety factor to have an idea whether a structure can be considered safe towards a certain collapse mechanism.

The introduced analytical models are based on the overturning and vertical flexural behaviour collapse mechanisms. In particular, the overturning scenario was analysed both for a 1-storey and a 2-storey building, while the vertical flexural behaviour was considered for a 2-storey building. Each scenario is studied twice: one configuration assuming that there is no connection among the involved macro-elements and another one that provides for an effective connection. The resulting six models were applied to two case studies, a 1-storey and a 2-storey building both collapsed during the 2016 Central Italy earthquake. Results highlight the importance of an efficient connection between the reinforced concrete roof and masonry walls and that some configurations are unsafe, which means additional investigations and possibly retrofit intervention are required. To account for the uncertainties introduced by the simplified models, sensitivity analyses were performed. These allowed to evaluate the influence of each input parameter to the overall safety level of the structure, highlighting peculiar aspects in each mechanism. Nonlinear kinematic analyses were also carried out and results were compared to those obtained from linear analyses. It was possible to observe that the linear analysis is faster and more precautionary as it provides smaller safety factors with respect to the nonlinear one.

Overall, the proposed analytical models represent an effective yet simple tool that can serve as a preliminary evaluation of the safety level of masonry structures retrofitted with reinforced concrete roofs. The method is not meant to be an alternative to other more refined analyses, such as finite element methods, that would allow for a more accurate safety verification. However, due to its simplicity, the procedure could be recommended when only few input data are available and be applied even by non-professional users to understand if further investigations and/or retrofit interventions are needed.

Acknowledgement

The research leading to these results has received funding from the European Research Council under the Grant Agreement n. ERC_IDEAL RESCUE_637842 of the project IDEAL RESCUE_Integrated Design and Control of Sustainable Communities during Emergencies.

References

[1] "DM 16-01-1996. Norme tecniche per le costruzioni in zone sismiche". 1996. Ministero dei Lavori Pubblici: Gazzetta Ufficiale.

[2] Calderini, C. 2008. "Use of reinforced concrete in preservation of historic buildings: conceptions and misconceptions in the early 20th century". *International Journal of Architectural Heritage*, 2(1): 25-59.

[3] Dolce, M., A. Masi, and A. Goretti. 1999. *Damage to buildings due to 1997 Umbria-Marche earthquake*. Seismic Damage to Masonry Buildings, ed. A. Bernardini. Leiden: A a Balkema Publishers. 71-80.

[4] Donati, S., F. Marra, and A. Rovelli. 2001. "Damage and ground shaking in the town of Nocera Umbra during Umbria-Marche, central Italy, earthquakes: The special effect of a fault zone". *Bulletin of the Seismological Society of America*, 91(3): 511-519.

[5] "DM 14-01-2008. Norme tecniche per le costruzioni". 2008. Ministero dei Lavori Pubblici: Gazzetta Ufficiale.

[6] "Circolare 2 febbraio 2009, n. 617 Istruzioni per l'applicazione delle «Nuove norme tecniche per le costruzioni»". 2009. Ministero delle Infrastrutture e dei Trasporti.

[7] Chen, Z.X., et al. 2016. "Nonlinear Analysis of Masonry Buildings Under Seismic Actions with a Multifan Finite Element". *International Journal of Structural Stability and Dynamics*, 16(1).

[8] Valente, M. and G. Milani. 2016. "Non-linear dynamic and static analyses on eight historical masonry towers in the North-East of Italy". *Engineering Structures*, 114: 241-270.

[9] Milani, G. 2011. "Simple lower bound limit analysis homogenization model for in- and out-of-plane loaded masonry walls". *Construction and Building Materials*, 25(12): 4426-4443.

[10] Milani, G. and M. Valente. 2015. "Comparative pushover and limit analyses on seven masonry churches damaged by the 2012 Emilia-Romagna (Italy) seismic events: Possibilities of non-linear finite elements compared with pre-assigned failure mechanisms". *Engineering Failure Analysis*, 47: 129-161.

[11] Arcidiacono, V., G.P. Cimellaro, and J.A. Ochsendorf. 2015. “Analysis of the failure mechanisms of the basilica of Santa Maria di Collemaggio during 2009 L'Aquila earthquake”. *Engineering Structures*, 99: 502-516.

[12] Arcidiacono, V., et al. 2016. “The Dynamic Behavior of the Basilica of San Francesco in Assisi Using Simplified Analytical Models”. *International Journal of Architectural Heritage*, 10(7): 938-953.

[13] Casapulla, C. and A. Maione. 2011. “Out-of-plane local mechanisms in masonry buildings. the role of the orientation of horizontal floor diaphragms”. *Proceedings of the 9th Australasian Masonry Conference*: 225-235.

[14] Costa, A.A., et al. 2012. “Out-of-plane behaviour of existing stone masonry buildings: experimental evaluation”. *Bulletin of Earthquake Engineering*, 10(1): 93-111.

[15] Guadagnuolo, M., A. Donadio, and G. Faella. 2012. *Out-of-plane failure mechanism of masonry building corners*. Structural Analysis of Historical Constructions, Vols 1-3., ed. J. Jasienko. Structural Analysis of Historical Constructions, Vols 1-3. 481-488.

[16] Makris, N. 2014. “The role of the rotational inertia on the seismic resistance of free-standing rocking columns and articulated frames”. *Bulletin of the Seismological Society of America*, 104(5): 2226-2239.

[17] Makris, N. and M.F. Vassiliou. 2014. “Dynamics of the rocking frame with vertical restrainers”. *Journal of Structural Engineering*, 141(10): 04014245.

[18] Giresini, L., M. Fragiacomo, and M. Sassu. 2016. “Rocking analysis of masonry walls interacting with roofs”. *Engineering Structures*, 116: 107-120.

[19] Borri, A., G. Castori, and A. Grazini. 2009. “Retrofitting of masonry building with reinforced masonry ring-beam”. *Construction and Building Materials*, 23(5): 1892-1901.

[20] Guadagnuolo, M. and G. Faella. 2015. “Floor masonry beams reinforced by BFRG Innovation on advanced composite materials for strengthening of masonry structures”, in *XIII Forum Internazionale di Studi “Le Vie dei Mercanti”–HERITAGE and TECHNOLOGY MIND KNOWLEDGE EXPERIENCE*. La scuola di Pitagora editrice, pp. 2108-2115.

[21] Fayala, I., O. Limam, and I. Stefanou. 2016. “Experimental and numerical analysis of reinforced stone block masonry beams using GFRP reinforcement”. *Composite Structures*, 152: 994-1006.

[22] Derakhshan, H., et al. 2014. “In situ out-of-plane testing of as-built and retrofitted unreinforced masonry walls”. *Journal of Structural Engineering*, 140(6): 04014022.

[23] Boscato, G., et al. 2014. “Seismic Behavior of a Complex Historical Church in L'Aquila”. *International Journal of Architectural Heritage*, 8(5): 718-757.

[24] Casapulla, C. and L.U. Argiento. 2016. “The comparative role of friction in local out-of-plane mechanisms of masonry buildings. Pushover analysis and experimental investigation”. *Engineering Structures*, 126: 158-173.